THE JOURNAL OF PHYSICAL CHEMISTRY C

Article

Modification of Solar Energy Harvesting in Photovoltaic Materials by Plasmonic Nanospheres: New Absorption Bands in Perovskite Composite Film

Krystyna Kolwas, and Anastasiya Derkachova

J. Phys. Chem. C, **Just Accepted Manuscript** • DOI: 10.1021/acs.jpcc.6b12140 • Publication Date (Web): 13 Jan 2017

Modification of Solar Energy Harvesting in Photovoltaic Materials by Plasmonic Nanospheres: New Absorption Bands in Perovskite Composite Film

Krystyna Kolwas* and Anastasiya Derkachova

Institute of Physics, Polish Academy of Sciences,

Al. Lotników 32/46, 02-668 Warsaw, Poland

E-mail: krystyna.kolwas@ifpan.edu.pl

Abstract

Thin-film perovskite-based photovoltaics has a great potential to make an important contribution to the ongoing search for new sources of clean renewable energy. Excitation of localized surface plasmons in metal nanoparticles could establish a new route for an improvement of the performance of such devices. Using the tools of electrodynamics (Lorenz-Mie theory adopted for absorbing host media), we predict a strong red-shift in spectral activity of gold and silver nanospheres and modification (negative or positive) of white and solar light harvesting in the film of perovskite host caused by centrally distributed plasmonic nanospheres. The enhancement of absorption in perovskite host is proven to be possible for photons with energies close to or smaller than the energy bandgap in perovskite, with the final effect depending on the diameter of nanospheres, their concentration and kind of metal. From the electronic band structure point of view, the predicted strengthening of absorption can be interpreted as the effect of semiconductor doping with metals resulting in increased photocurrent. New allowed energy bands within the bandgap of the undoped perovskite semiconductor, allow explaining the recently observed effect of boosted photocurrent generation (Nano Lett. 2013, 13, 4505 and Adv. Funct. Mater. 2015, 25,5038).

1 Introduction

Thin-film photovoltaics has the great potential to make an important contribution to the ongoing search for new sources of clean renewable energy. However, solar cells based on the photovoltaic effect in practice display much lower conversion efficiencies than a theoretical maximum of about 32% due to the Shockley-Queisser limit.[1] One of the reasons is that the solar cell bandgap and a solar spectrum do not fully coincide. Another limitation in all thin-film solar cell technologies is that their absorbance of near-bandgap light is ineffective.

Excitation of localized surface plasmons in metal nanoparticles could open a route to increase the performance of photovoltaic devices. In general, plasmonic excitations give rise

to a variety of effects which can be tuned by their size and shape, such as absorption and scattering spectra or strong electromagnetic field concentration and enhancement that occurs in the vicinity of metal surface (see, e.g.,[2–5] for reviews). Strong interaction of such nanoparticles with light makes them efficient receiving or/and scattering optical nanoantennas with tunable optical properties.[6–9] The large optical cross sections of metal nanoparticles at wavelengths corresponding to their plasmon resonance make them potentially very attractive for a variety of applications that include harvesting solar energy. Excitation of surface plasmons in nanoparticles embedded in semiconductor might be expected to enhance absorption of incident photons within the semiconductor region near each nanoparticle, as well as redirect light into the semiconductor increasing the absorption path-length. Such effects could enhance photocurrent response (see[10–13] and references therein). Moreover, the radiative coupling of a plasmons with an excitons in a semiconductor is expected to influence radiative recombination of electron-hole pairs and improve the photocurrent by increasing the optical pathway for light reemitted from electron-hole pairs recombination.[14,15]

In semiconductors, photon energies in excess of the threshold energy (the gap between valence and conduction bands) are usually dissipated as heat, so that this absorbed photon energy often is expected to do no useful work. However, recent studies (e.g.[13,16–19]) reveal the new possibilities for hot-carrier harvesting that may allow power conversion efficiencies beyond the Shockley-Queisser limit by implementing hot-carrier technology. In that context, hot charge carrier extraction from metallic nanostructures offers also a very promising prospects for applications (see[20–24] and references therein). e.g., in photovoltaics. Plasmon excitations in metallic nanostructures can be engineered to enhance and provide valuable control over emission of such hot-carriers.

In the past few years the photovoltaic field has experienced extremely dynamic increase due to development of perovskite-based photovoltaic devices[14,18,25–29] that are expected to be the next generation solar cells. Hybrid perovskites display relatively high power conversion efficiencies due to their absorbing characteristics, which include long carrier lifetimes, and a

significant defect tolerance for solution-processed polycrystalline films. However, absorption by perovskites (as well as by other photovoltaic materials[12,18,30,31]) of solar radiation at longer wavelengths is not optimal.

Spherical nanoparticles such as gold and silver nanospheres are plasmonic structures of particular potential interest for solar light harvesting applications,[12,14,15,32–34] since their spherical geometry allow for effective interaction with incident light of any polarization,[35] as well as with unpolarized light. Their plasmonic characteristics are well known when embedded in nonabsorbing media like air. In case of nonabsorbing host media, plasmonic activity of gold and silver nanoparticles falls in the spectral range of sunlight. When illuminated by light wave of frequency, which matches the spectral region of their characteristic size-dependent resonance frequencies,[5,9,36,37] nanoparticle's optical cross-section becomes much higher than the geometrical cross-section. For nonabsorbing host media, such cross-sections can be predicted on the base of electromagnetic description known as the Lorenz-Mie theory, which can be found in several monographs (e.g.[3,38–40]). Extensions of the Lorenz-Mie theory are known for multilayered spheres[41–43] and for arbitrary incident light beams.[44] However, in many cases of practical importance the Lorenz-Mie theory in its original formulation fails due to the fact that the host medium is absorbing. When ignored (e.g., some commercial computational codes for calculating the absorption or extinction cross-sections), the results obtained formally after applying complex index of refraction for the medium are wrong. In particular, it happens that the extinction in some frequency ranges becomes negative. To describe correctly the absorbing and scattering spectra of nanospheres embedded in absorbing hosts (e.g. perovskite), an appropriate description is required.

The main aim of the present study is to assess a modification of the absorption spectra in a thin-film absorbing materials resulting from admixture of plasmonic spherical nanoparticles of various sizes using a rigorous electrodynamic modeling (near-field effect and retardation effects taken into account). First, the explicit spectral absorbing and scattering characteristics of gold and silver nanoparticles of various size embedded in thin-film perovskite are given.

Farther, the lower limit of the modification of absorption spectrum of perovskite host by the plasmonic particles of various sizes is assessed. Finally, the net modification of the spectrum of absorbed energy in the perovskite material alone is considered. Several spectral measures of such modification are introduced, and the possible absorption enhancement is studied as a function of nanoparticle size. The issue of whether plasmon excitations in gold and silver nanospheres can enhance absorption of photovoltaic thin-film materials is discussed in two spectral regions corresponding to energies below and over the energy bandgap in perovskite.

The presented model can be applied for any thin-film of absorbing materials containing nanospheres. However, in all the calculations we use the example of thin-film perovskite containing gold and silver nanospheres of various radii. Optical properties of perovskite under consideration are assumed to be described by the dispersion relation data of methylammonium lead triiodide perovskite $CH_3NH_3PbI_3$ (MAPI) deposited on a (100) silicon wafer (for details see[45,46]), in the wavelengths range from $300nm$ to $1500nm$. The perovskite thin-film is assumed to be 300nm thick. Originally, all the example spectra are calculated for flat spectral illumination of the film. Later, all the results are recalculated for sunlight illumination. Finally, the role of nanospheres size in generating the favorable conditions for enhancing the absorption of perovskite host (and photocurrent generation) is discussed. All the basic electrodynamic considerations, which are the integral part of our study, have been shifted to Appendices section.

2 Optical properties of photovoltaic thin-films embedding plasmonic nanoparticles; basis of modeling

Let us consider a composite thin-film of thickness h made of homogeneous absorbing (photovoltaic) material with embedded spherical particles of radius R (Figure 1). The N plasmonic particles of the same radius R are distributed over the film volume along the central plane of the film with a mean distances d between particles.

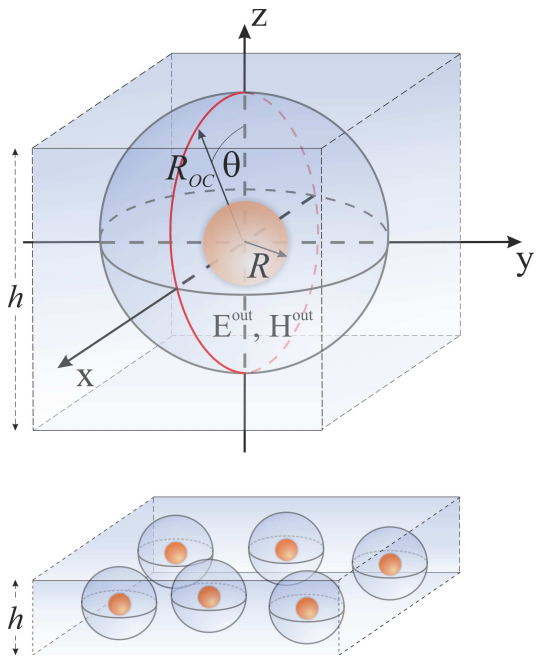

Figure 1: Illustration of the concept of the optical cell (OC) of diameter $2R_{OC} = h$, containing the central plasmonic nanosphere of radius R. The filling factor of the film of thickness h by OCs depends on the concentration n_v of plasmonic nanoparticles

To determine the macroscopic optical properties of a bulk medium in which many small particles are immersed, it is commonly assumed that distances between particles are larger than the light wavelength.[47] In such case scattering by one particle can be considered independent of scattering by another. In the considered case of nanoparticles (NPs) embedded in an absorbing film, this condition can be weakened due to presence of absorption in the medium. If distances between the particles are smaller, multiple scattering of light is more effective and absorption in the host medium is enhanced. Therefore, assuming independent scattering of light by immersed particles in the farther modeling, we possibly underestimate the absorption in a host rather. Assuming electromagnetically independent plasmonic particles, one should recall stricter condition related to plasmon coupling. In a nonabsorbing media it is usually assumed that plasmon coupling can be neglected when $d > 5R$.[48] In absorbing hosts this condition is expected to be even weaker. Therefore, if we assume plasmonic optically uncoupled nanospheres of diameters up to $2R = 150nm$, distanced $d \geq h = 300nm$, we do not overestimate the possible enhancement of absorption in the absorbing host mate-

rial.

We assume that absorbing host material is optically homogeneous and characterized by a wavelength dependent complex refraction index $n(\lambda_0)$, where λ_0 is the free-space wavelength of light wave illuminating the film. Permeabilities of the materials are assumed to be unity. The perovskite composite thin-film, which we consider in all numerical calculations for illustrating our modeling, is composed of methylammonium lead triiodide perovskite $CH_3NH_3PbI_3$, and gold or silver nanoparticles. Let us note that the available data sets delivering $n(\lambda_0)$ for perovskites vary depending on the source. In case of thin-film photovoltaic devices such as thin-film solar cells, the dispersion data for active material can be additionally affected by presence of materials applied in fabricating the solar cell architecture. Perovskite CH3NH3PbI3 deposited on a (100) silicon wafer[45,46] was chosen to represent the host for the nanopartciles in the numerical calculations. Let us note that the maximum of the imaginary part of the index of refraction $\mathrm{Im}[n(\lambda_0)]$ for perovskite, which defines the absorptive properties of the material, does not coincide with the maximum of the sunlight spectrum (see Fig. 2). The complex indexes of refraction $n_{in}(\lambda_0)$ accepted for gold and silver inclusions comes from.[49]

In our modeling we assume the incident light beam to be already in the active film (details of the description in Sections A1 and A2 of the Supplementary Materials). Thus we omit all energy losses caused by reflection and refraction on the sides of the film. We neglect also an interaction of nanospheres with the back reflected light beams, the effect, which would increase absorption of reflected light if present in a strongly absorbing film. One can state that this assumption (and all other assumptions we have made) leads to underestimation of the absorption in an absorbing (photovoltaic) material under study.

2.1 The concept of the elementary optical cell of composite film

In order to describe all the near-field optical processes in an elementary volume of the composite material of a fixed thickness, we introduce the concept of elementary optical

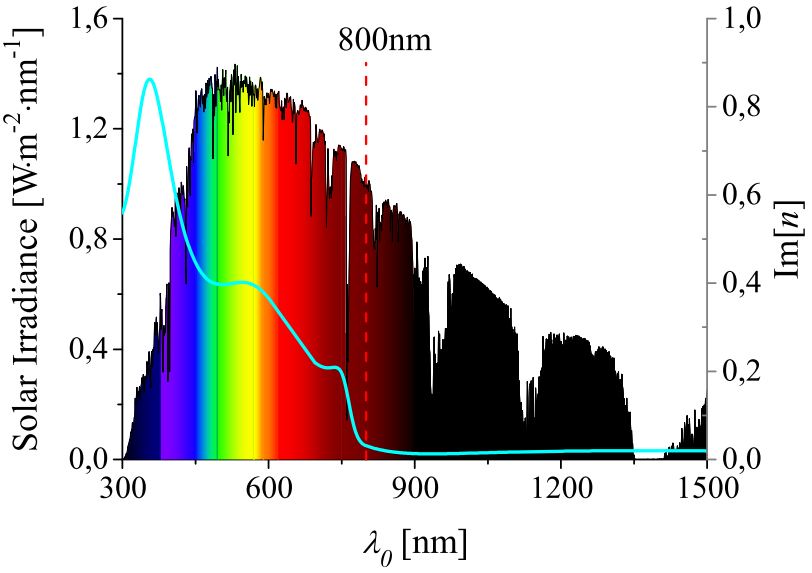

Figure 2: Imaginary part of the index of refraction of organic-inorganic hybrid perovskite $CH_3NH_3PbI_3$ deposited on a (100) silicon wafer as a function of wavelength according to the data from RefractiveIndex.INFO base[46] (right axis). On the background: the spectrum of sunlight, according to[50]

cell. Due to the spherical symmetry of the plasmonic particle, it is natural to consider the spherical elementary optical cell (OC) of the diameter $2R_{OC}$ composed of the absorbing material (with the complex index of refraction n), and the plasmonic nanosphere (with the complex index of refraction n_{in}) in the center (see Fig. 1). Spherical symmetry of OC allows adopting the general concept of Lorenz-Mie theory in order to find the exact electromagnetic (EM) fields inside and outside the central spherical particle (SP) and use them to account for the modification of absorption in the absorbing host material caused by presence of the plasmonic nanosphere. Considering the modification of optical properties of the composite film by SPs, it would be more appropriate to consider an elementary cube of length edge h (see Fig. 1), or, even better, N elementary cuboids of height h filling the volume of the film. However, mathematical complexity of the description favors the choice of a spherical OC. Considering N elementary spherical OCs of the diameter $2R_{OC} = h$, we can be sure that the estimated modification of the absorption of host material contained in the OC is not overestimated in comparison with the corresponding quantity for N elementary cuboids.

Considering the elementary spherical OC of radius $R_{OC} = 150nm$ cut from the thin-film perovskite composite of thickness $h = 300nm$ (see Figs. 1 and A1 b)) (see Section A1 of Supplementary Materials for more details), we find all necessary quantities that contribute to the modification of spectral properties of the composite film and host absorbing material. Systems, which we must examine in order to account for absorption in the host material in presence of SP, are the following (see Fig. 3 a)-c)): i) the sphere of volume V_{OC} filled with the absorbing material, circumscribed by the surface $\mathbf{\Sigma}_{OC}$ (Fig. 3 a)), ii) the whole OC of volume V_{OC} circumscribed by the surface $\mathbf{\Sigma}_{OC}$ with the particle in the center, iii) the central particle (of volume V circumscribed by the surface $\mathbf{\Sigma}$) in the absorbing host (Fig. 3 b)), and iv) the hollow absorbing sphere of volume $V_{OC} - V$ circumscribed by the surface $\mathbf{\Sigma}_{OC}$ (Fig. 3 c)). Varying the radius R of SP we can study the role of SP size in shaping the spectra of absorbed energy in the whole OC, and finally in the material hosting the SP.

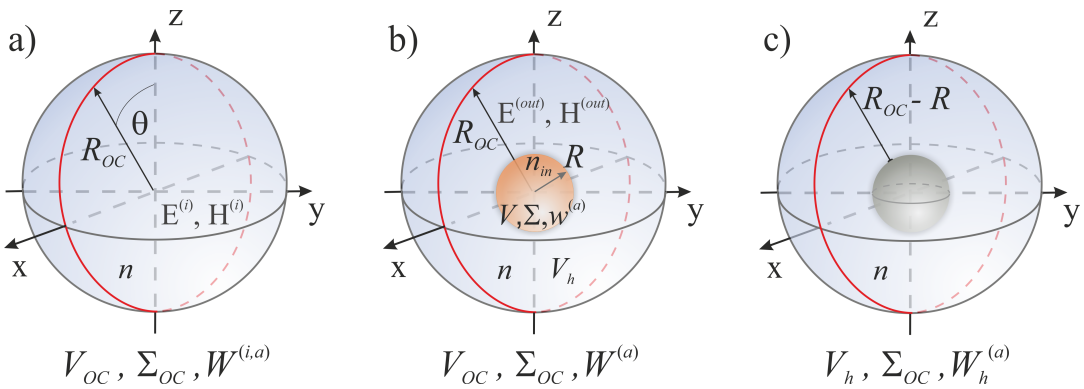

Figure 3: Illustration of the optical systems, which have been considered in the modeling: a) the absorbing (perovskite) sphere of volume V_{OC} (of radius R_{OC}) without plasmonic inclusions (absorption rate: $W^{(i,a)}$), b) the optical cell of volume V_{OC} (absorption rate $W^{(a)}$), composed of absorbing material (perovskite) and central plasmonic particle of volume V (absorption rate $w^{(a)}$), c) the absorbing host layer (perovskite) of volume $V_h = V - V_{OC}$ embedding the particle (absorption rate $W_h^{(a)}$ in presence of plasmonic particle)

2.2 Lorenz-Mie scattering theory for a sphere in absorbing medium

Lorenz-Mie scattering theory, developed for a sphere embedded in a nonabsorbing medium (e.g.[38,39]), treats strictly the scattering of EM radiation by spheres of arbitrary size and yields

well known expressions for EM fields in the sphere and its dielectric environment, angular intensity distribution of scattered light as well as scattering and extinction cross-sections. In the case of absorbing host, the generalization of this formalism must be used, in order to take into account the effect of absorption in the medium. Such generalization, using a far-field approximation for the EM fields, proposed in,[51] would not be appropriate even as a starting point for the case studied here, as the near-field effects are crucial. Our modeling is based in part on the results of the previous papers,[51–56] especially those presented in,[52,53] which are considered as a generalization of[51] for near-field effects. In,[53,55] inherent and apparent cross-sections for absorption, scattering and extinction of a nanosphere were introduced in order to get the quantities which do not depend on the radius of integration sphere or the absorption in the host medium. However, in all these works the effort was focussed on the optical properties of a sphere, and not on the modification of the optical properties of the host medium be the particle, which is our aim. Another problem which we encountered in these papers and to which we refer in Section A3.2 in more details, is related to the meaning of extinction cross-section.

But the most meaningful problem from the point of applicability of the results[51–56] to our problem (and to other problems of practical importance) is the fact, that in these papers all studied quantities are parametrized by the amplitude E_c of the incident field defined in the center of integration sphere (in the center of SP) and independent on the intensity spectrum of light at the illuminated border of the absorbing materials. In our approach (see Sections A1 and A2 of the Supplementary Materials for details), $|E_0|^2$ is used as the external parameter of the modeling. E_0 is the amplitude of harmonic plane wave with the wavelength λ_0 and intensity I_0 illuminating the film (see Fig. A1 a)). Therefore, all the studied spectra become proportional to the intensity of illuminating light I_0 with wavelength $k_0 = 2\pi/\lambda_0$ (see eq. (A9)) at the illuminated border of the absorbing film. That allows us to introduce any spectral profile of illuminating light.

2.3 Summary of basic concepts of the modeling

We assume that the elementary optical cell (OC) of the composite film composed of the absorbing host and the central plasmonic nanospheres accounts for all processes of basic importance for modification of the absorption of the absorbing film hosting the plasmonic spherical particle (SP). The cell with the diameter corresponding to the thickness of composite film h (see Fig. 1) is inscribed in the center of an elementary cuboid of the height h and the length depending on the number density of SPs. N such cuboids fill the volume of the composite film. Modification in the absorbed energy introduced by plasmonic SP in the host material of OC is not overestimated in comparison with the corresponding quantity in an elementary cuboid. In the numerical calculations we assume that the thickness of the composite film is $h = 300nm$, the film is illuminated by a plane wave with the intensity I_0 proportional to $|E_0|^2$. We put $|E_0|^2 = 1V^2/m^2$ (flat spectral illumination) or we introduce the solar spectrum $I_0 = I_0(\lambda_0)$.[50] The film is composed of perovskite with optical properties defined by the complex index of refraction $n(\lambda_0)$[45] and of admixed gold or silver spherical inclusions of optical properties defined by the complex index of refraction $n_{in}(\lambda_0)$.[49] The inclusions are uniformly distributed in the central plane along the illuminated film surface with distances $d > h$. The problem is solved for particles of radii R from $10nm$ up to $150nm$ with the step $\Delta R = 10nm$.

3 Scattering and absorption spectra of gold nanoparticles in thin perovskite film illuminated with light of flat free-space profile

Noble metal nanoparticles embedded in nonabsorbing media exhibit absorption and scattering cross-sections far exceeding their geometrical cross-section in the spectral region of their characteristic size-dependent plasmon resonance frequencies. In case of nonabsorbing host

media, plasmonic activity of gold NPs fall in the visible spectral range of sunlight, while in case of silver it is shifted toward UV-violet range, depending on the NPs size and dielectric properties of the embedding material.[5,9,37]

In the absorptive media, the corresponding scattered $w^{(s)}$ and absorbed $w^{(a)}$ energy rates are modified in shape and strength to the extend resulting not only from the dispersion, but also from the absorption of the incident light in the host, which is dependent on the propagation length. Therefore, in case of the fixed thin-film thickness, the optical path changes with the particle size. In our modeling we take these effects into account.

The details of the basis of electrodynamic description of spectral characteristics of NPs in absorptive environment have been shifted to Section A3 of Supplementary Materials. Using eqs. (A15), (A20) and expressing the central value $|E_c(\lambda_0)|^2$ in these formulas by $|E_0(\lambda_0)|^2$ of the light wave illuminating the film (eq. (A13)), we get the spectra of energy rates absorbed $w^{(s)}(\lambda_0)$ and scattered $w^{(a)}(\lambda_0)$ by SPs in the film of thickness h. For completeness, we find the corresponding scattering $w'^{(s)}(\lambda_0)$ and absorbed $w'^{(a)}(\lambda_0)$ spectra for the same particles embedded in the nonabsorbing host calculated within the standard Lorenz-Mie theory (Subsection A3.3).

Figures 4 and 5 show, how the absorbing film of perovskite influences the spectra of rates of scattered $w^{(s)}(\lambda_0)$ and absorbed $w^{(a)}(\lambda_0)$ energy by gold and silver SPs of various radii, in comparison with the corresponding rates of energy $w'^{(s)}(\lambda_0)$ and $w'^{(a)}(\lambda_0)$ in nonabsorbing host ($n = 1$). The absorption spectra of gold SPs in the perovskite film are much wider than in case of nonabsorbing host and, what is the most interesting, these spectra are strongly shifted toward larger λ_0. Their shape is deformed by the absorption of the incident light in the host.

The scattering and absorption spectra $w^{(s)}(\lambda_0)$ and $w^{(a)}(\lambda_0)$ of gold and silver SPs presented in Figures 4 b) and 5 b) are centrally embedded in the perovskite composite film of thickness $h = 300nm$. The film is illuminated with light of flat free-space spectral profile of intensity proportional to $|E_0|^2$. $w^{(s)}(\lambda_0)$ and $w^{(a)}(\lambda_0)$ energy rates increase dramatically

with the diameter of SP, as demonstrated for the sequence of $2R$ starting from 10nm up to 150nm. Maximum spectral activity of larger gold and silver plasmonic NPs falls just below and over $\lambda_0 = 800nm$, the wavelength corresponding to the energy bandgap in perovskite host. In this spectral range, $\mathrm{Im}[n(\lambda_0)]$ for perovskite (see Fig. 2) is small (in the range $\lambda_0 \leq 800nm$), or negligible ($\lambda_0 > 800nm$). Large SPs are more efficient scatterers than absorbers. In principle, this feature can favour the increase in the total absorption rate in perovskite host in case of larger SPs.

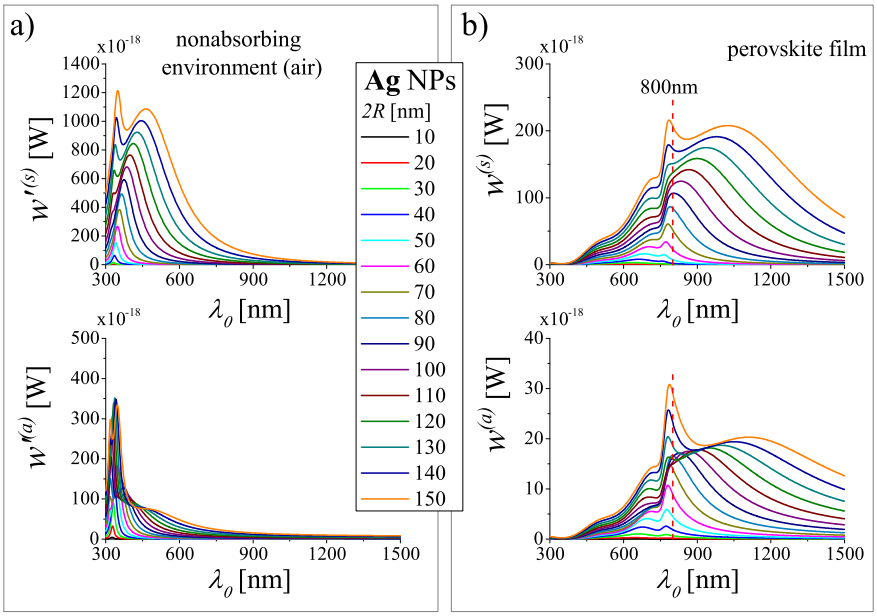

Figure 4: Spectra of scattered and absorbed energy rates of silver spherical NPs for a sequence of diameters a) in air and b) centrally embedded in the perovskite film

Comparison of $w^{(s)}(\lambda_0)$ (see Fig. 6) for gold (dashed line) and silver SPs (solid line) embedded in perovskite film leads to the conclusion that smaller Ag SPs are better scatterers of radiation energy than the corresponding Au SPs in the low wavelength range, where the perovskite absorption is maximal (see $\mathrm{Im}[n(\lambda_0)]$ in the range $300nm < \lambda_0 < 450nm$ in Fig. 2). Gold SPs effectively scatter light at larger wavelengths λ_0 of the light illuminating the film.

Absorption of radiation energy by metal NPs (top graphs in Figs. 4, 5) within plasmonic mechanism is expected to heat the nanoparticle due to the ohmic losses in a metal. Such

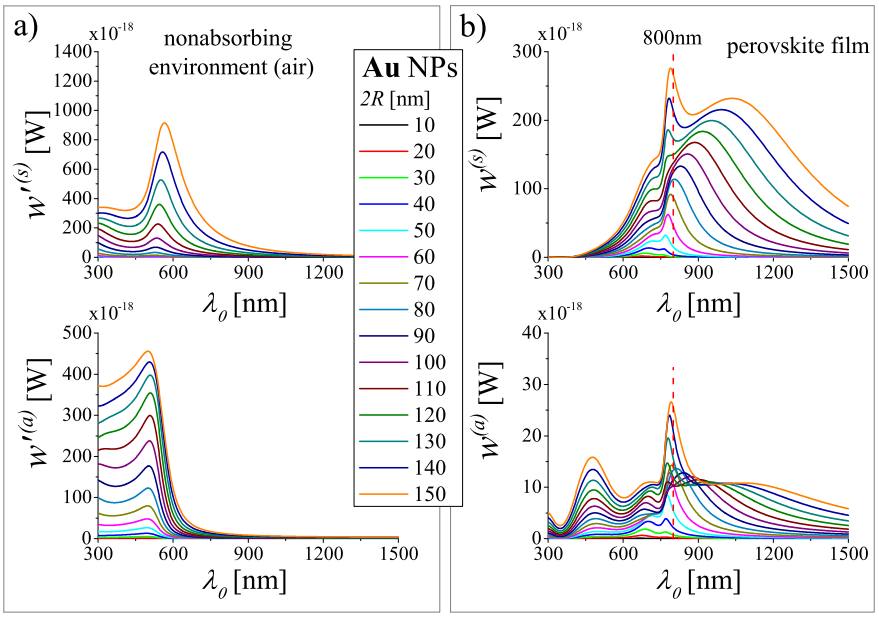

Figure 5: Spectra of scattered and absorbed energy rates of gold spherical NPs for a sequence of diameters a) in air and b) centrally embedded in the perovskite film

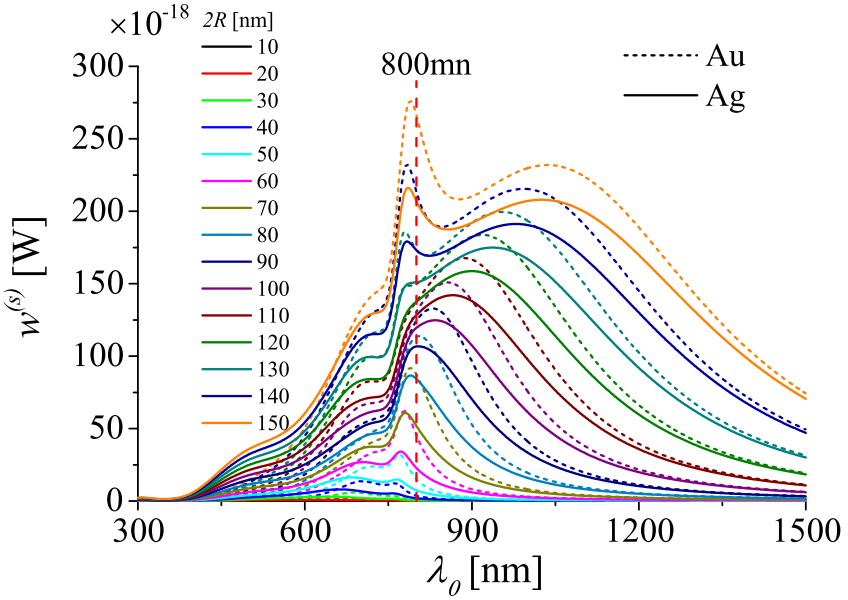

Figure 6: Comparison of spectra of scattered energy rates of gold (dashed line) and silver spherical NPs (solid line) embedded in perovskite film, for various diameters of NPs

picture applies better to Ag than to Au SPs.[9,13] Effectiveness of the heating process can be accounted by the size dependence of the nonradiative plasmon damping rates contributing to the total plasmon damping rates.[8,13]

4 Spectra of energy rates absorbed and removed by the optical cell of the composite perovskite film

The rate $W^{(a)}$ of the total energy absorbed by the optical cell of radius R_{OC} (see Fig. 3 b)) can be expressed as an integral of the radial component of the time-averaged Poynting vector over the surface $\mathbf{\Sigma}_{OC}$ which envelopes the volume V_{OC} filled by absorbing material (perovskite) and the central (plasmonic) particle (see Fig. 3 b) and Section A4 of the Supplementary Materials for details). The rate of the total energy $W^{(a)}$ absorbed in OC can be expressed as the sum of the terms (eq. (A31)):

$$W^{(a)} = W^{(i,a)} - W^{(s)} + W', \tag{1}$$

where $W^{(i,a)}$ is the rate of absorption of the incident beam by the absorbing material (perovskite), which fills the whole volume V_{OC} in absence of a scattering particle (see Fig. 3 a)), $W^{(s)}$ is the rate of energy scattered out by the SP and reaching the border of the OC (after propagating in the absorbing medium). The term W' has no self-reliant physical meaning like in the case of nonabsorbing host medium (see Subsection A4.3 for more details), but it contributes to the total rate of energy $W^{(ext)}$ removed by OC.

After calculating the integrals defining $W^{(i,a)}$, $W^{(s)}$, W' (see Section A4), it is possible to find the total absorption rate $W^{(a)}$ (eq. 1). In spite the task is algebraically rather hard, all the terms $W^{(i,a)}$, $W^{(s)}$ and W' can be calculated strictly (see eqs. (A34), (A36) and (A38) in Section A4). Spectra of the terms contributing to $W^{(a)}$) (eq. (1)), the resulting absorption

spectra $W^{(a)}(\lambda_0)$ and the extinction spectra $W^{(ext)} \equiv W^{(a)} + W^{(s)}$ calculated as the sum $W^{(i,a)} + W'$ are illustrated in the following subsections for divers diameters of gold and silver SPs embedded in perovskite film.

4.1 Spectrum of absorption of the incident beam in absence of scattering particle

Fig. 7 illustrates the spectrum of absorbed energy rate $W^{(i,a)}(\lambda_0)$ in perovskite, which fills the spherical volume V_{OC} (in absence of a scattering particle) after illumination of the perovskite film of thickness $h = 300nm$ with light of flat free-space spectral profile (dotted line) and sunlight (solid line). $W^{(i,a)}(\lambda_0)$ is the strong nonlinear function of wavelength λ_0, due to the interplay of dependencies $I_c(\lambda_0)$, $n(\lambda_0)$ and $\eta(\lambda_0) = 4\pi R_{OC}\,\mathrm{Im}[n(\lambda_0)]/\lambda_0$ (eq. (A34)). $W^{(i,a)}$ is also dependent on the choice of the radius R_{OC} and, therefore, on the thickness of composite film h, as we have assumed $2R_{OC} = h$.

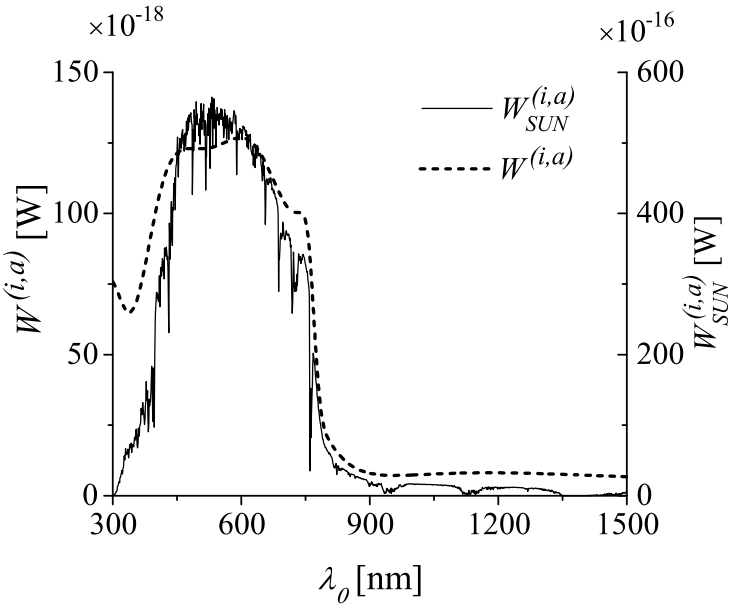

Figure 7: Spectrum of energy rate absorbed by the perovskite sphere of volume $V_{OC} = (4/3)\pi R_{OC}^3$ in case the film is illuminated with light of flat spectral profile ($E_0 = 1V^2/m^2$, left axis, dashed line) and with solar light (right axis, solid line)

4.2 Scattered spectra

Figure 8 (solid lines) illustrates spectral dependence of $W^{(s)}(\lambda_0)$ for the sequence of diameters of gold and silver SPs (solid lines) embedded in perovskite after illumination of perovskite film with thickness $h = 300nm$ with light of flat free-space spectral profile. All $W^{(s)}(\lambda_0)$ spectra fall into the visible range near the band-gap limit (at 800nm) and extend over that limit to the infrared range. Dashed lines illustrate the corresponding spectra of energy rates $w^{(s)}(\lambda_0)$ scattered by the central gold or silver particle, before propagation in the host. The difference in both quantities below the wavelength corresponding to the energy band-gap is quite large, while for larger wavelengths it is much smaller due to very weaker absorption of perovskite in this spectral range (see $\mathrm{Im}[n(\lambda_0)]$ in Fig. 2).

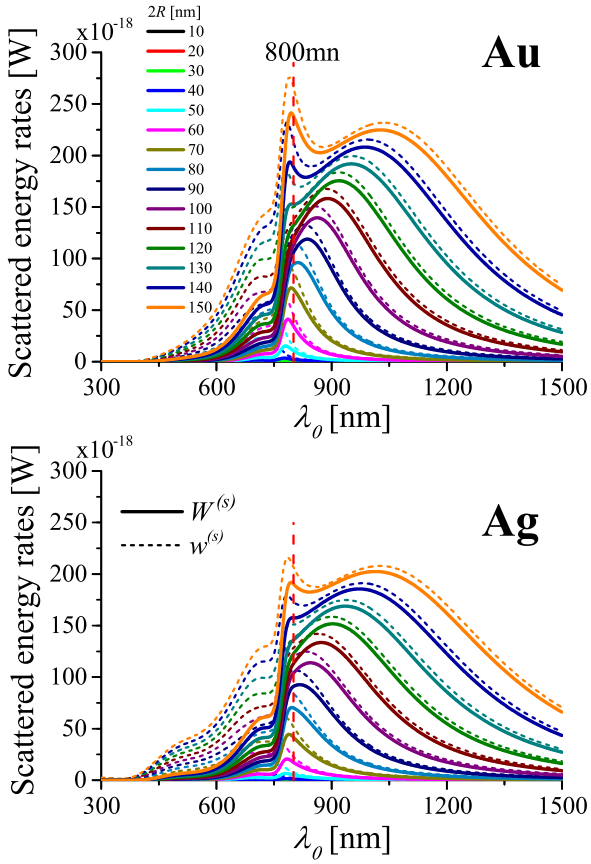

Figure 8: Spectra of energy rates $w^{(s)}(\lambda_0, R)$ (dotted lines) scattered by plasmonic NPs, and the corresponding spectra $W^{(s)}(\lambda_0, R)$) (solid lines) at the surface of the optical cell after travelling in perovskite host

Let us note that while the OC is embedded in the perovskite film (see Figs. 1), energy scattered by the nanosphere propagates still outside OC borders, contributing to the enhanced absorption in the perovskite. Therefore, absorption of the scattered energy in the film is larger than those estimated by $W^{(s)}$ for the perovskite contained in the OC.

4.3 Extinction spectra

Figure 9 illustrates $W'(\lambda_0)$ (eq. (A38)) spectra (dotted lines) for gold and silver SPs of various diameters, embedded in perovskite host, after illumination of the film of thickness $h = 300nm$ with light of flat free-space spectral profile. W' (eq. (A37)) has no self-reliant physical meaning like in the case of nonabsorbing host medium (see Subsection A4.3), but it contributes to the total rate of energy removed by OC. Figure 9 illustrates the extinction spectrum $W^{(ext)}(\lambda_0)$ (solid lines) (eq. (A39)), calculated as the sum of $W^{(i,a)}$ and W' (see Section A4.3 for more details). Note that $W'(\lambda_0)$ spectra became slightly negative for some frequency ranges (inset in Fig. 9), contrary to $W^{(ext)}(\lambda_0) \equiv W^{(a)}(\lambda_0) + W^{(s)}(\lambda_0)$. Extinction of the illuminated composite film can be measured experimentally.

4.4 Absorption spectra

$W^{(i,a)}(\lambda_0)$, $W^{(s)}(\lambda_0)$ and $W'(\lambda_0)$ spectra contribute to the spectra of the total energy $W^{(a)}(\lambda_0)$ absorbed in the whole OC (eq. (1)) in presence of SP of diameter $2R$. Fig. 10 a) illustrates the spectral dependence of $W^{(a)}(\lambda_0)$ for a sequence of diameters of gold and silver SP embedded in perovskite, after illumination of perovskite film of thickness $h = 300nm$ with light of flat free-space spectral profile.

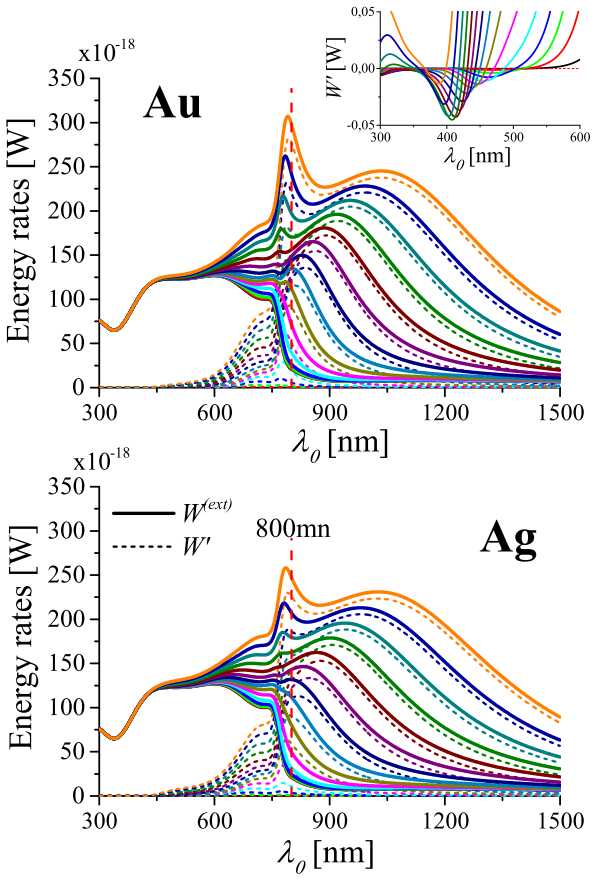

Figure 9: Spectra of energy rates $W^{(scat)}(\lambda_0, R)$ removed from the incident light (solid lines) and those of $W'(\lambda_0, R)$ (dashed lines) for gold and silver spherical NPs embedded in perovskite host. The inset demonstrates that $W'(\lambda_0, R)$ can take the negative values

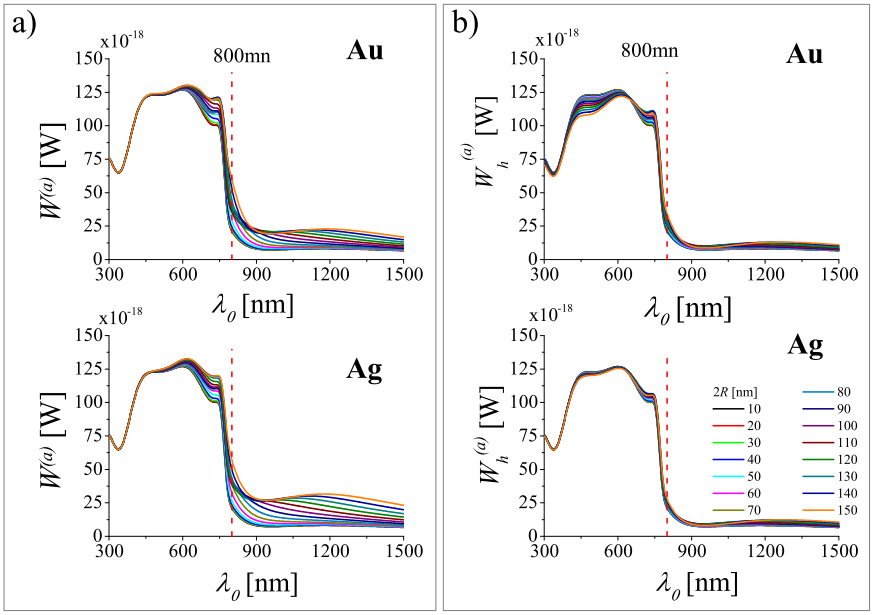

Figure 10: Comparison of spectral dependence of energy rates absorbed a) $W^{(a)}(\lambda_0, R)$ - by the whole optical cell (host and NP) and b) $W_h^{(a)}(\lambda_0, R)$ - in a layer of perovskite host embedding the gold and silver NPs of various diameters

5 Spectral modification of absorption in perovskite by plasmonic particles in the elementary optical cell

5.1 Spectral net modification of absorption in perovskite host by plasmonic particles after illumination by spectrally flat light and sunlight

The absorption rate $W^{(a)}$ of the whole OC (eq. (1)) must be the sum of the rates: $w^{(a)}$ absorbed by the particle in the absorptive host (eqs. (A15)) and $W_h^{(a)}$ absorbed in the host in presence of the particle: $W^{(a)} = w^{(a)} + W_h^{(a)}$. Therefore, the total rate $W_h^{(a)}$ of energy absorbed in the SP's surrounding (within the volume $V_h = V_{OC} - V$, see Fig. 3 c)) in presence of SP, is the difference of quantities which we just know (see Subsection 4.4 or Section A4 for more details):

$$W_h^{(a)} = W^{(a)} - w^{(a)}. \quad (2)$$

Fig. 10 b) illustrates the spectra of rates of energy $W_h^{(a)}(\lambda_0)$ absorbed in the layer of perovskite host embedding the gold or silver SP for a sequence of sizes, after illumination of perovskite film of thickness $h = 300nm$ with light of flat free-space spectral profile. The rates $W_h^{(a)}(\lambda_0)$ are the quantities of interest in photovoltaic applications; the net rate of energy absorbed in the host medium (and not the total rate of energy absorbed in a composite) relates to the photocurrent generation in active photovoltaic material. Comparing Fig. 10 a) and b) one can state that the contribution of absorption $w^{(a)}$ in a plasmonic particle (which is turned mainly into heat), introduces important, size dependent contribution to the modification of the total energy rate $W^{(a)}$ absorbed by OC, which is the measurable quantity.

To access the direct effect resulting from incorporation of plasmonic SPs to the photovoltaic material, we consider the net change $\Delta W_h^{(a)}(\lambda_0)$ in the rate of absorbed energy by the host medium, resulting from presence of plasmonic particle:

$$\Delta W_h^{(a)} = W_h^{(a)} - W^{(i,a)}, \quad (3)$$

where as before: $W_h^{(a)}$ is the energy rate absorbed in the hosting material in OC in presence of SP and $W^{(i,a)}$ is the rate of energy absorbed by that material in case it fills the whole volume of OC (SP is not present). If in some spectral range $\Delta W_h^{(a)}(\lambda_0) > 0$, absorption of photovoltaic material is reinforced.

Having in mind possible photovoltaic applications, we recalculated all the quantities contributing to $\Delta W_h^{(a)}(\lambda_0)$ (eq. (3)) by replacing the previously assumed flat free-space spectrum of light illuminating the film by sunlight spectrum[50,57] (see Section A5 for more details). Figure 11 summarizes our results concerning the spectral modification of the absorption $\Delta W_h^{(a)}(\lambda_0)$ and $\Delta W_{h,SUN}^{(a)}(\lambda_0)$ of perovskite host resulting from admixture of gold

or silver nanospheres of various radii R for a) spectrally flat and b) sunlike illumination of the composite film correspondingly. Evidently, modification of absorption $\Delta W_h^{(a)}(R)$ and $\Delta W_{h,SUN}^{(a)}(\lambda_0)$ is much more efficient for larger particles. The depletion of absorption takes place for shorter λ_0 from the studied spectral range, while the maximal reinforcement of absorption falls for wavelengths just below $\lambda_0 = 800nm$, corresponding to the bandgap in perovskite. The depletion is much more pronounced for a composite containing gold inclusions than silver ones. Important enhancement of $\Delta W_h^{(a)}(\lambda_0)$ and $\Delta W_{h,SUN}^{(a)}(\lambda_0)$ falls in the spectral range, where perovskite without plasmonic admixtures weakly absorbs light (see $\mathrm{Im}[n(\lambda_0)]$ in Fig. 2), with the spectrally wide part falling above $\lambda_0 = 800nm$ (photon energies smaller than $\sim 1.55eV$, well below the perovskite energy bandgap). Note that absorption in perovskite (without SPs) in this spectral range does not lead to the increase in photocurrent.

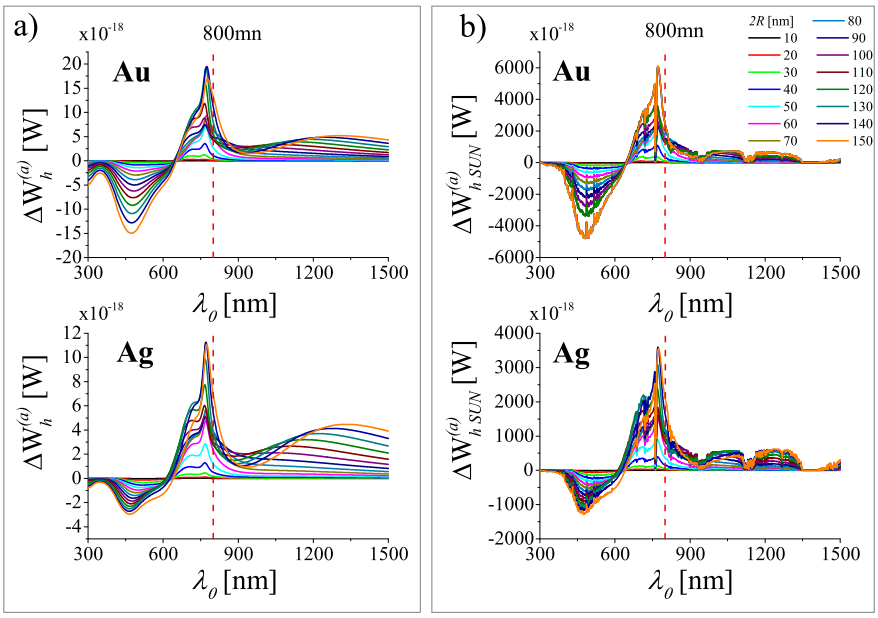

Figure 11: Net change in the spectra of absorbed energy rates in the perovskite host, resulting from presence of gold or silver NPs of various diameters, after illumination of perovskite composite film a) with light of flat free-space spectral profile, b) with sunlight

The spectral measures of the modification of light harvesting by plasmonic SPs which we have introduced, apply to the nanometer-sized volume of a single elementary OC. When related to the extended composite thin-film with $2R_{OC} = h$, the effect of many admixed

NPs adds in the volume of the film occupied by the OCs. So, the final gain or depletion of spectral absorption in the photovoltaic material (perovskite) introduced by presence of NPs, increases with the concentration n_v of the NPs. For example, if one takes $n_v \approx 3.7 \cdot 10^{13} cm^3$, the number of NPs in the film of surface $s = 1cm^2$ is $n_v hs = N_{OC} \approx 10^9$. Therefore, the expected single-OC spectral effects will be larger by nine orders of magnitude in the whole volume of the composite film occupied by the OCs.

5.2 Relative spectral modification of absorption in perovskite host by plasmonic particles after illumination by sunlight

$\Delta W^{(a)}_{h,SUN}(\lambda_0)$ related to the rate $W^{(i,a)}_{SUN}$ allows assessing the relative spectral modification of the absorbed energy in the perovskite host resulting from presence of SP of radius R:

$$M(\lambda_0, R) = \frac{\Delta W^{(a)}_{h,SUN}(\lambda_0, R)}{W^{(i,a)}_{SUN}(\lambda_0)}\%. \tag{4}$$

Such parameter defines the important measure for the objective assessment of the spectral modification of absorbing (photovoltaic) materials by admixture of plasmonic SPs of various radii in the OC.

Figure 12 illustrates the relative spectral modification $M(\lambda_0)$ of absorption in perovskite by gold and silver SPs of various diameters $2R$. Negative effect occurs for shorter wavelengths (for photons energies exceeding the energy bandgap), and is larger for gold than silver nanoparticles. Positive modification $M(\lambda_0)$ achieves several dozen percent of the energy absorbed by the perovskite without admixture for larger plasmonic inclusions. Enhancement occurs in the spectral range near and above $\lambda_0 = 800nm$, with the spectrally narrower maximum near the energy bandgap and with the wide maximum for photon energies smaller than $\sim 1.55eV$ (in red and infrared regions) below the perovskite bandgap, in the range where absorption in the perovskite without metal NPs can not contribute to the photocurrent generation (Fig. 13).

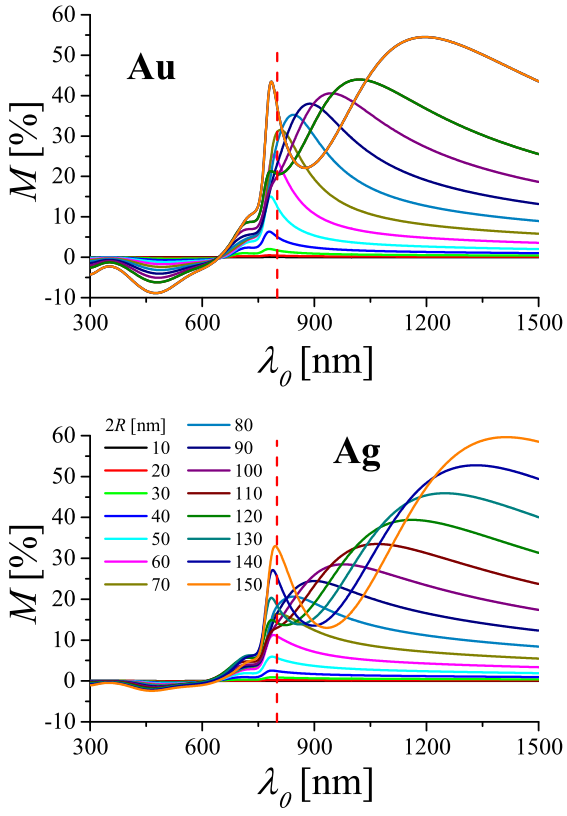

Figure 12: Relative modification in the spectrum of absorbed energy, resulting from presence of a) gold or b) silver NPs in the perovskite host, related to the spectrum of absorption in perovskite in case the NPs are not present

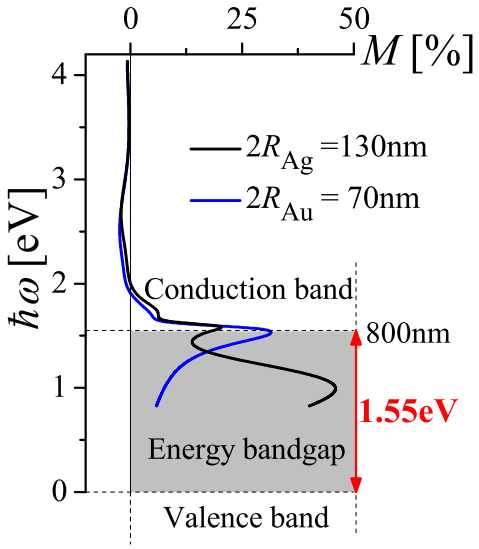

Figure 13: Modification M of the absorption energy spectra (in percent) of the perovskite host, resulting from presence of gold and silver NPs of chosen diameters versus the scheme of the energy bands of perovskite without NPs.

The revealed important positive relative spectral modification $M(\lambda_0)$ of absorption by incorporation of metal NPs is the most important result of our study, with the fundamental consequences for photocurrent enhancement. The predicted modification of absorption of photons in the "forbidden" energy band of perovskite (Fig. 13) is expected to be reflected in change of conductive properties of composite. Such enhanced absorption can be assigned to the new absorbing bands of doped perovskite and, as we expect, it can lead to the gain in photocurrent generation.

6 Integral modification of absorption in perovskite by plasmonic particles in the elementary optical cell

In order to get the generalized measure of potential usefulness of plasmonic NPs in improving light harvesting of perovskite composite film (and their photovoltaic performance), we introduce the integral spectral modification of absorption in perovskite host $\Delta W^{(a)}_{h,SUN}\left[{}^{\lambda\max}_{300nm}\right]$ and the corresponding integral measure $M^{\lambda\max}_{300nm}$. $\Delta W^{(a)}_{h,SUN}\left[{}^{\lambda\max}_{300nm}\right]$ adds up positive and negative changes in the absorption rate $\Delta W^{(a)}_{h,SUN}(\lambda_0)$ (eq. (3) for sunlight illumination) in the spectral range under study:

$$\Delta W^{(a)}_{h,SUN}(R)\left[{}^{\lambda\max}_{300nm}\right] = \int_{300nm}^{\lambda\max} d\lambda_0 \left[\Delta W^{(a)}_{h,SUN}(\lambda_0, R)\right]. \tag{5}$$

The corresponding relative integral measure, with respect to the total radiation energy $\int_{300nm}^{\lambda\max} d\lambda_0 W^{(i,a)}_{SUN}(\lambda_0)$ absorbed by the host filling the whole volume of the OC in absence of SPs, can be expresses as:

$$M^{\lambda\max}_{300nm}(R) = \frac{\Delta W^{(a)}_{h,SUN}(R)\left[{}^{\lambda\max}_{300nm}\right]}{\int_{300nm}^{\lambda\max} d\lambda_0 W^{(i,a)}_{SUN}(\lambda_0)}\%. \tag{6}$$

The relative integral spectral modifications $M^{\lambda\max}_{300nm}$ of the absorption by the SPs is the essential parameter of our study. It allows estimation of the potential improvement (or

defeat in case of $M < 0$) of thin-film plasmonic composite for building photovoltaic devices (in comparison with the case where NPs are not incorporated), in the spectral range of interest (in our case from 300nm up to the chosen λ max).

In case of perovskite host, we will consider two spectral ranges of wavelengths respectively: i) the full studied spectral range up to λ max $= 1500nm$, ii) up to λ max $= 800nm$. The absorption of photons from the second spectral range only $(300nm - 800nm)$ leads to a standard photocurrent generation in perovskite of absorptive properties unaffected by NPs. Figure 14 shows both: $M_{300nm}^{1500nm}(R)$ (line with black empty squares) and $M_{300nm}^{1500nm}(R)$ (line with blue empty spheres).

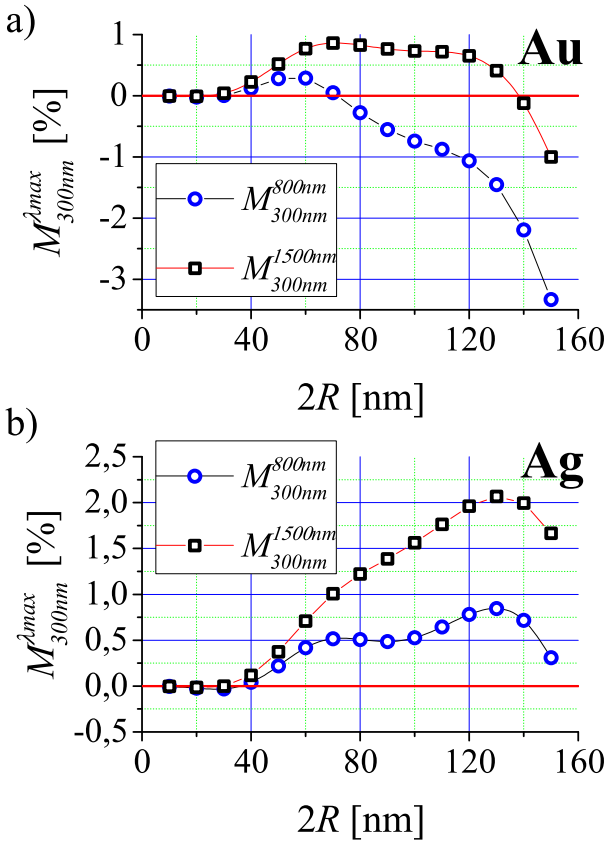

Figure 14: Modification (positive or negative) of the integrated spectra of the total absorbed energy (in percent) in the perovskite host, resulting from presence of a) gold and b) silver NPs of various diameters. Lines with black empty squares show $M_{300nm}^{1500nm}(R)$, after integration over the full studied spectral range, while lines with blue empty spheres shows $M_{300nm}^{800nm}(R)$, after integration over the spectral range, where the gain in the absorption in perovskite without NPs is expected to enhance photocurrent

In case of gold NPs (Figure 14 a)), when considering only the absorption in the spectral range $300nm - 800nm$ (empty spheres), positive modification ($M_{300nm}^{800nm}(R) > 0$) does not exceed 0,3%. Very modest enhancement of light harvesting by incorporation of gold NPs of diameters from the narrow range of about $35nm - 70nm$ only is expected. Admixture of larger gold NPs leads to important negative modification of absorption in perovskite. Admixture of silver NPs (empty spheres in Figure 14 b)) is expected to be more favorable: the integrated relative enhancement of light harvesting is expected for NPs of diameters from about $40nm$ (to the end of studied size range) with $M_{300nm}^{800nm}(R)$ approaching or exceeding 0,5%, with the maximum 0,85% for $2R = 130nm$.

However, when considering the modification of absorption in the full spectral range from $300nm$ to $1500nm$ (line with black squares in Fig. 14), the total enhancement of absorption in perovskite host becomes much more pronounced in case of larger SPs, reaching the optimum of 2% for Ag SPs of diameter of about 130nm. As demonstrated, from the point of view of its plasmonic properties, inclusion of large silver SPs is more profitable than of gold ones. Opposite is true in case of their chemical activity as gold NPs are known to be more inert.

7 Summary and Conclusions

Our study was motivated by recent extremely dynamic development of perovskite-based photovoltaic devices with their great potential to be applied in next generation solar cells. The presented model allows assessing enhancement of light harvesting in active materials of absorbing films by admixture of plasmonic nanospheres. We introduced several measures of such modification resulting in the gain and depletion of absorption in the host (perovskite) material in the spectral range from 300nm to 1500nm. Rigorous electrodynamic description that we applied allowed us to accounts for modification of plasmonic characteristics of the nanosphere by the absorbing host, and vice versa. The model can be applied for any film of absorbing materials containing any optically uncoupled, centrally distributed nanospheres.

As an example, all the calculations were made for thin-film perovskite film of thickness 300nm and gold and silver spherical nano-inclusions with diameter within the 10nm-150nm range.

In order to account for the near-field optical processes in the nano-thin film composite, we used strict electromagnetic theory (based on Maxwell's equations) and energy budget equations (based on Pointing theorem) applied to the elementary (spherical) optical cell cut from the composite film. Such cell consists of a central plasmonic (gold or silver) nanosphere and an absorbing host (perovskite). Considering N such cells with the diameter equal to the thickness of the film, we can be sure that the estimated modification of the energy absorbed in the active material of the film filled with the optical cells, is not overestimated in comparison with the corresponding quantity for N elementary cuboids containing the cell. Lorenz-Mie theory extended for spheres immersed in an absorbing host medium allowed us to describe absorption of the primary electromagnetic fields propagating in the absorbing host together with those scattered by the nanosphere. Absorption by the nanosphere was also accounted for. External parameters of our model include spectral parameters of the light illuminating the film.

Initially, we found the absorption and scattering spectra of gold and silver nanospheres of various sizes embedded in the perovskite film, the spectra of total absorption and extinction rates of plasmonic optical cell, and finally, the net energy rates absorbed by the host material (perovskite) in presence of a plasmonic particles of various sizes. At this stage, all the spectra were calculated for flat spectral illumination of the film with the amplitude of the illuminating plane wave assumed to be $1V^2/m^2$. Finally, all the spectra were recalculated for illumination of the film by a sunlike light.

Optical activity of plasmonic nanoparticles is strongly affected by absorbing host. The spectral absorbing and scattering characteristics of gold and silver nanoparticles of various size, hosted by the thin-film perovskite, are red-shifted in comparison with the corresponding spectra for particles in air. Maximal spectral activity of larger gold and silver plasmonic

particles falls in the range just below and over $\lambda_0 = 800nm$, the wavelength corresponding to the energy bandgap in perovskite. In this spectral range, perovskite (without plasmonic admixtures) absorbs light weakly. Larger nanoparticles are more efficient scatterers than absorbers. In the low wavelength (UV) range, silver nanospheres scatter light more effectively than the corresponding gold nanospheres. In turn, gold nanospheres are more efficient absorbers in this frequency range. A significant component of the total absorbed energy is turned into heat in the plasmonic particle. Our analysis proves that structuring the photovoltaic thin films according to the simplified criterion of maximal absorption by the film containing plasmonic inclusions is incorrect.

Moreover, the role of plasmonic nanospheres in modifying the spectral characteristics of the host material was considered as a function of particle's size. We introduced several measures of such modification, which describe the gain and depletion of absorption in the host (perovskite) material in the spectral ranges from 300nm to 1500nm and from 300nm to 800nm as a function of particle's size. Modification of the absorption spectra in the perovskite host is size dependent and much more efficient for larger particles.

The depletion of absorption takes place for shorter wavelengths of the studied spectral range and is more pronounced for a composite containing large gold nanoparticles (up to $8,87\%$ for $\lambda_0 = 473$) than containing silver ones (up to $2,41\%$ for $\lambda_0 = 466nm$).

The most important finding of this work is the predicted reinforcement of light harvesting in the perovskite host in the spectral range, where, when undoped, it can not absorb radiation. The enhancement of absorption in perovskite host is proven to be possible for photons with energies close to or smaller than the energy bandgap in perovskite, with the final effect depending on the diameter of nanospheres, their concentration and kind of metal (Fig. 12). The enhancement of the relative absorption (related to the absorption in the volume in case the nanoparticles are not incorporated) takes place in the range corresponding to the energy bandgap limit $\sim 1.55eV$ (see Fig. 13) of perovskite (narrower maximum near λ_0 =800nm) and extends towards lower energies (the second broad maximum in red and infrared regions).

Maximum absorption gain reaches 50% or 60% for largest diameters (150nm) depending on the metal (Au or Ag) and fall in near infrared part of the spectrum. As we expect, the spectrally narrower contribution to the gain with the maximum below λ_0 can significantly influence both the luminescence and photocurrent enhancement, while the part of the wide absorption band over λ_0 =800nm can lead to the increased photocurrent.

In addition, we introduced the total spectral measure of potential usefulness of plasmonic nanospheres in improving the performance of perovskite films for photovoltaics. The integral spectral modification of absorption in the perovskite host (caused by presence of plasmonic particles) adds up positive and negative changes in the absorption rate in the corresponding spectral ranges. Using this measure, we can state that large silver nanoparticles are better candidates as doping agents for photovoltaic perovskite cells than the gold ones. Their integrated action in enhancing the absorption can be positive in both studied spectral ranges: from 300nm to 800nm and from 300nm to 1500nm. Absorption in the former range is known to result in photocurrent generation in undoped perovskite. Absorption in the latter range, revealed contribution from new absorption bands which appear directly as a result of semiconductor doping with metal nanoparticles. The optimal size of silver nanospheres for boosting performance of plasmonic perovskite solar cell is expected to range from 80nm to 160nm, with the maximum of the enhancement for the diameter 130nm. In practical realization of plasmonic solar cells, the core-shell nanoparticles are usually used, what leads to slight modification of the optimal size and diminution of the expected positive effect. However, in the attempt of boosting the efficiency of solar energy conversion, the single percent of increase counts.

New absorption bands predicted by our model can shed a new light on the experiments applying core-shell nanoparticles incorporated into perovskite-based solar cells (see experimental results[14,15] on the role of $Au@SiO_2$ (80nm diameter) and $Ag@TiO_2$ (40nm diameter)). In case of gold nanoparticles, the authors unambiguously observed enhanced photocurrent, but no significant change to the white-light harvesting capability in the studied wavelength

spectral range, which have been limited (in both cases of $Au@SiO_2$ and $Ag@TiO_2$ nanoparticles) to the spectral range below 800nm. Therefore, the absorption to the energy band(s) of the doped perovskite (over 800nm) predicted by our model have not been observed. But, as we expect, such previously unpredicted absorption was the main reason of the observed photocurrent enhancement.

The predicted enhancement of light harvesting by incorporation of metal nanoparticles can be understand as the effect of semiconductor doping, which results in a behaviour more similar to a conductor's one with all consequences for the new allowed energy levels (bands) and boosting photocurrent. Our electrodynamic modelling of this effect opens new way in predicting the enhancement of solar conversion efficiency in photovoltaic materials.

8 Appendices

A1 Absorption of electromagnetic energy in a spherical volume - the basis

The net average rate ΔW at which EM energy passes trough the surface $\mathbf{\Sigma}$ which bounds the volume V is given by the surface integral (e.g.[44,58])

$$\Delta W = -\oint_{\mathbf{\Sigma}} \langle \mathbf{S} \rangle \cdot \widehat{\mathbf{n}}\, da, \tag{A1}$$

where $\widehat{\mathbf{n}}$ is an outward unit vector normal to the surface, da is an infinitesimal area of the surface, and $\langle \mathbf{S} \rangle$ is the time average of the Poynting vector $\mathbf{S}(\mathbf{r},t) = \frac{1}{\mu_0}[\mathrm{Re}\,\mathbf{E}(\mathbf{r},t) \times \mathrm{Re}\,\mathbf{B}(\mathbf{r},t)]$. If $\langle \mathbf{S} \rangle$ represents the directional mean energy flux density of $exp(i\omega t)$-harmonic EM fields:

$$\langle \mathbf{S}(\mathbf{r}) \rangle = \frac{1}{T}\int_0^T \mathbf{S}(\mathbf{r},t)\, dt = \frac{1}{2}\,\mathrm{Re}[\mathbf{E}(\mathbf{r}) \times \mathbf{H}^*(\mathbf{r})]\,, \tag{A2}$$

where the star denotes a complex conjugate. For a nonabsorbing medium (media) which

fills the volume V, the incoming energy is balanced by the outgoing energy and $\Delta W = 0$. But when the volume V is filled with the absorbing material(s), $\Delta W \neq 0$ and it represents now the total rate at which the EM energy is being absorbed in the volume confined by the surface $\mathbf{\Sigma}$. The absorbed electromagnetic energy is transformed into other forms of energy (e.g. heat) by a process not described by EM theory.

If the absorbing volume V is a sphere, the absorbed energy rate $\Delta W = W^{(a)}$ is represented by the integral of the radial component $\langle S_r \rangle$ of $\langle \mathbf{S} \rangle$, taken over the sphere surface:

$$W_{sph}^{(a)} = \int_0^{2\pi} \int_0^{\pi} \langle S_r(r_{sph}, \theta, \varphi) \rangle \, da, \tag{A3}$$

where $da = r_{sph}^2 \sin\theta d\theta d\phi$ is an infinitesimal surface area and r_{sph} is the sphere radius. To find $\langle S_r \rangle$, it is sufficient to consider the transverse components of the EM fields $\mathbf{E}(\mathbf{r})$ and $\mathbf{H}^*(\mathbf{r})$ which in the spherical coordinate system (r, θ, φ) are expressed by series of spherical multipole partial waves, similarly to their counterparts in the case of conventional Mie formulation for nonabsorbing host media. Let us note that the validity of relationship A1 is not restricted to the case of a homogeneous material contained in the volume V.

A1.1 Incident fields in the absorbing material without inclusions

The incident light wave, assumed to be already in the host medium,[51–56] is polarized in the direction of x axis in the Cartesian coordinate system (x, y, z), selected to be at the center of the sphere, with the positive $z = R_{OC} \cos\theta$ axis along the direction of propagation (see Fig. A1). The space dependent part of electric and magnetic fields of this wave propagating in the absorbing material of the film (see Fig. 3 a)) can be written as:

$$\mathbf{E}^{(i)}(x,y,z) = \widehat{\mathbf{e}}_x E_c \exp\left(ik_0 \operatorname{Im}[n]\, z\right), \tag{A4}$$

$$\mathbf{B}^{(i)}(x,y,z) = \frac{\operatorname{Re}[n]}{c} \nabla \times \mathbf{E}^{(i)}(x,y,z) = \tag{A5}$$

$$= \widehat{\mathbf{e}}_y \frac{\operatorname{Re}[n]}{c} E_c \exp\left(ik_0 \operatorname{Im}[n]\, z\right), \tag{A6}$$

where $k_0 = \omega/c = 2\pi/\lambda_0$, c is the speed of light in vacuum, $\widehat{e}_x$ and $\widehat{e}_y$ are the unit vectors along the x and y axes, respectively, and n is the refractive index of the absorbing material (perovskite). $\mathbf{B} = \mu_0 \mathbf{H}$, while we assume the magnetic permeability of the material to be unity. E_c is the amplitude of electric field at $z = 0$, which in[51–56] have been used as the given, external parameter of the description, common for all wavelengths λ_0 of the illuminating light waves.

The incident irradiance i.e., the magnitude of time-averaged Poynting vector $\langle \mathbf{S}^{(i)} \rangle$ (eq. (A2)) is then:

$$\langle \mathbf{S}^{(i)} \rangle = \widehat{\mathbf{e}}_z I_c \exp\left(-2k_0 \operatorname{Im}[n] z\right), \tag{A7}$$

where I_c (eq. (A11)) is the irradiance of incident radiation in the central plane of the absorbing film at $z = 0$ (see Fig. A1 a)).

A1.2 Fields in the composite material

Intensity of the incident light is not only attenuated when propagating in the host material of the composite, but is also partially scattered and absorbed by the central NP. Light, which is scattered by NP, is also attenuated when propagating in the absorbing host. Following the scheme of Lorenz-Mie theory (e.g.[38]), the EM fields satisfying Maxwell's equations in the host medium surrounding the central scattering particle, may be represented as the sum of the incident field (assumed to be already in the cell) and the scattered field:

$$\mathbf{E}^{out}(\mathbf{r}) = \mathbf{E}^{(i)}(\mathbf{r}) + \mathbf{E}^{(s)}(\mathbf{r}), \quad \mathbf{H}^{out}(\mathbf{r}) = \mathbf{H}^{(i)}(\mathbf{r}) + \mathbf{H}^{(s)}(\mathbf{r}) \tag{A8}$$

at any point $\mathbf{r} = (r, \theta, \phi)$, with r: $R < r \leq R_{OC}$. Let us note that the fields $\mathbf{E}^{(i)}$ and $\mathbf{H}^{(i)}$ in eq. (A8) are solutions of Maxwell's equations in absence of the particle. $\mathbf{E}^{in}(\mathbf{r})$ and $\mathbf{H}^{in}(\mathbf{r})$ $(0 < r \leq R)$ denote solutions of Maxwell's equations for the fields inside the particle. The corresponding fields fulfil standard continuity relations across the interface at $r = R$. Therefore, $\mathbf{E}^{out}$ and $\mathbf{H}^{out}$ fields outside the particle (and also at the surface Σ_{OC}) take into account the presence of the central SP. In spherical coordinates the expansions of incident and scattered fields $\mathbf{E}^{out}, \mathbf{H}^{out}, \mathbf{E}^{in}, \mathbf{H}^{in}$ are similar to their counterparts in the case of conventional Lorenz-Mie formulation (e.g.[38]), but the complex, wavelength dependent refractive index of the absorptive sphere surroundings is used.

A2 Propagation of incident radiation in the absorbing film without plasmonic inclusions

If the absorbing film with the complex index of refraction n is illuminated by harmonic plane wave (see Fig. A1 a)) with the amplitude E_0 and wave number $k_0 = \omega/c = 2\pi/\lambda_0$ (c is the speed of light in vacuum), the intensity of the incident light in the absorbing material on the illuminated side of the film is proportional to $|E_0|^2$:

$$I_0 = \frac{\mathrm{Re}[n]}{2c\mu_0}|E_0|^2 = \frac{k_0\,\mathrm{Re}[n]}{2\omega\mu_0}|E_0|^2. \tag{A9}$$

In the film's material intensity of light is attenuated exponentially with the wavelength dependent coefficient $2k_0\,\mathrm{Im}[n(\lambda_0)]$ starting from I_0 value at the illuminated surface of the film ($z' = 0$, see Fig. A1 a)): $I^{(0)}_{film}(z') = I_0 \exp[-(k_0 n)z']$. In the system of coordinates $(x, y, z = z' - h/2)$ shifted to the center of the film it can be presented as:

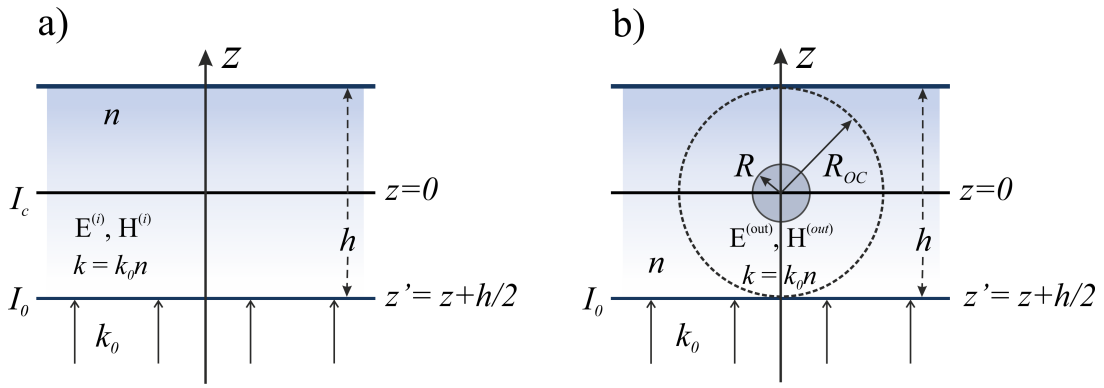

Figure A1: Geometry of normal illumination of a) absorbing film of thickness h without inclusions and of b) absorbing composite film containing the centrally distributed plasmonic nanoparticles

$$I_{film}^{(0)}(z) = I_0 \exp[-(2k_0 \,\mathrm{Im}[n](h/2 + z))]. \tag{A10}$$

Therefore, the intensity I_c in the central xy plane of the film (at $z = 0$):

$$I_c = \frac{k \,\mathrm{Re}[n]}{2\omega\mu_0}|E_c|^2 = I_0 \exp(-\alpha) \tag{A11}$$

changes with the wavelength λ_0 of light illuminating the film and thickness h of the film:

$$\alpha(\lambda_0) = \frac{2\pi h \,\mathrm{Im}\,[n(\lambda_0)]}{\lambda_0}. \tag{A12}$$

While we consider the linear optical properties of the studied systems, all the processes scale with $|E_0|^2$ of the light wave (with the wavelength λ_0) illuminating the film. In particular, in the center of the film $|E_c|^2$ is wavelength dependent due to the absorption of the film and spectral distribution of the illuminating light:

$$|E_c(\lambda_0)|^2 = |E_0(\lambda_0)|^2 \exp\left(-\alpha(\lambda_0)\right), \tag{A13}$$

In the calculations in Sections 2.1-A3 we put $E_0 = 1V^2/m^2$ for all wavelengths λ_0 from the range from $300nm$ to $1500nm$, so we assume spectrally flat (white) illumination. However,

in general, we can define any spectral profile of the illuminating beam (e.g. that of the solar light) by varying $|E_0\lambda_0)|^2$ accordingly to the illuminating profile, as we do in Section 5 where we introduce the solar spectrum.

A3 Optical properties of nanospheres in absorptive environment

A3.1 Rate of energy absorbed by a nanosphere in the absorptive medium

The rate $w^{(a)}$ of energy absorbed in the volume V occupied by the SP of radius R, can be expressed (eqs. (A1, A2, A3)) as an integral of the radial component of the time-averaged Poynting vector over the surface $\mathbf{\Sigma}$ which envelopes the volume V of the SP (see Fig. 3 b)). The involved components of the fields satisfy standard continuity relations at the particle/host interface. Therefore, one can use either $\mathbf{E}^{out}(\mathbf{r}), \mathbf{H}^{out}(\mathbf{r})$ (scattered plus incident) fields, as usual, or the internal fields $\mathbf{E}^{in}(\mathbf{r}), \mathbf{H}^{in}(\mathbf{r})$ at $r = R$,[53] what makes integration simpler:

$$\begin{aligned} w^{(a)} &= -\frac{1}{2}\,\mathrm{Re}\oint_{\mathbf{\Sigma}}\left[\mathbf{E}^{in}\times\mathbf{H}^{in*}\right]_r ds = \\ &= \frac{1}{2}\,\mathrm{Re}\int_0^{2\pi} d\phi \int_0^{\pi}\left(E^{in}_{\varphi}H^{in*}_{\theta} - E^{in}_{\theta}H^{in*}_{\varphi}\right) R^2\sin\theta d\theta. \end{aligned} \tag{A14}$$

Profiting from the integration performed in,[53] the energy rate $w^{(a)}$ absorbed by a spherical particle embedded in the absorbing host reads:

$$w^{(a)} = \frac{\pi\,|E_c|^2}{\omega\mu_{in}}\sum_{l=1}^{\infty}(2l+1)\,\mathrm{Im}\,(A_l)\,, \tag{A15}$$

where the coefficient A_l:

$$A_l = k_{in}^{-1}\left[|c_l|^2\,\psi_l(x)\psi_l'^*(x) - |d_l|^2\,\psi_l'(x)\psi_l^*(x)\right], \tag{A16}$$

and $k_{in} = 2\pi n_{in}/\lambda_0$. The expressions for the scattering coefficients, c_l and d_l, are formally identical to the Mie coefficients inside the particle, obtained in the case of a non-attenuating host medium (see e.g.[38]):

$$c_l = \frac{m\xi_l(x)\psi_l'(x) - m\xi_l'(x)\psi_l(x)}{m\xi_l(x)\psi_l'(mx) - \xi_l'(x)\psi_l(mx)}, \tag{A17}$$

$$d_l = \frac{m\xi_l'(x)\psi_l(x) - m\xi_l(x)\psi_l'(x)}{m\psi_l(mx)\xi_l'(x) - \xi_l(x)\psi_l'(mx)}, \tag{A18}$$

where $k = 2\pi n/\lambda_0$, $x = kR$, λ_0 is the wavelength of incident light in vacuum, $m = n_{in}/n$, and Riccati-Bessel and Riccati-Hankel functions: $\psi_l(x) = xj_l(x)$, and $\xi_l(x) = xh_l^{(1)}(x)$ are defined by $j_l(x)$ and $h_l^{(1)}(x)$ Bessel and Hankel functions. Primes indicate the differentiation in respect to the argument. In all calculations we assume the media to be nonmagnetic: $\mu = \mu_{in} = \mu_0$.

A3.2 Rate of energy scattered by a nanosphere in the absorptive medium

The rate of energy scattered by a spherical particle $w^{(s)}$ is defined by the radial component of the corresponding Poynting vector:[38]

$$\begin{aligned} w^{(s)} &= \frac{1}{2}\,\mathrm{Re}\oint_{\mathbf{\Sigma}}\left[\mathbf{E}_s\times\mathbf{H}_s^*\right]_r ds = \\ &= \frac{1}{2}\,\mathrm{Re}\int_0^{2\pi} d\phi \int_0^{\pi}\left(E_{s\theta}H_{s\varphi}^* - E_{s\varphi}^{in}H_{s\theta}^*\right) R^2\sin\theta d\theta \end{aligned} \tag{A19}$$

which is defined by the fields $\mathbf{E}_s$, $\mathbf{H}_s$ scattered by the particle, and taken at $r = R$. Using the results of calculations performed in,[53] the energy rate scattered by a spherical particle embedded in the absorbing host is:

$$w^{(s)} = \frac{\pi |E_c|^2}{\omega\mu} \sum_{l=1}^{\infty} (2l+1) \operatorname{Im}(B_l), \tag{A20}$$

where the coefficient B_l is expressed by the scattering coefficients a_l and b_l, which are formally identical to those obtained in the case of a non-attenuating medium (see e.g.[38]):

$$B_l = k^{-1} \left[|a_l|^2 \xi_l'(x) \xi_l^*(x) - |b_l|^2 \xi_l(x) \xi_l'^*(x) \right] \tag{A21}$$

$$a_l = \frac{m\psi_l(mx)\psi_l'(x) - \psi_l(x)\psi_l'(mx)}{m\psi_l(mx)\xi_l'(x) - \xi_l(x)\psi_l'(mx)}, \tag{A22}$$

$$b_l = \frac{\psi_l(mx)\psi_l'(x) - m\psi_l(x)\psi_l'(mx)}{\psi_l(mx)\xi_l'(x) - m\xi_l(x)\psi_l'(mx)}. \tag{A23}$$

A3.3 Rates of energy scattered and absorbed by a nanosphere in the nonabsorbing medium

For completeness, the scattering $w^{(s)}(\lambda_0)$ and absorption $w^{(a)}(\lambda_0)$ spectra are compared with the corresponding scattering $w'^{(s)}(\lambda_0)$ and absorbed $w'^{(a)}(\lambda_0)$ spectra for the same particles embedded in the nonabsorbing host ($n = 1$, see Figures 4 a) and 5 a)). $w'^{(s)}(\lambda_0)$ and $w'^{(a)}(\lambda_0)$ energy rates for gold and silver SPs of various sizes have been calculated within the standard Lorenz-Mie theory:

$$w'^{(s)} = I_0 C_{scat}, \tag{A24}$$

$$w'^{(a)} = I_0 C_{abs}, \tag{A25}$$

where $C_{scat} = \pi R^2 Q_{scat}$ and $C_{abs} = \pi R^2 Q_{abs}$ are the total scattering and absorption

cross-sections for nanoparticles in a nonabsorbing environment, and Q_{scat} and Q_{abs} are the corresponding scattering and absorption efficiencies. The radius-dependent plasmon resonances contributing in various spectral regions to $C_{scat}(\lambda_0)$ and $C_{abs}(\lambda_0)$ can be identified. However, unambiguous size dependence of plasmon resonances spectral positions results from solving the dispersion relation for surface localized EM fields (see[8,9,37]).

A4 Total absorbed energy rates in the optical cell

The rate $W^{(a)}$ of energy absorbed by the optical cell of radius R_{OC} (see Fig. 3 b)) can be expressed as an integral of the radial component of the time-averaged Poynting vector over the surface $\mathbf{\Sigma}_{OC}$ which envelopes the volume V_{OC} filled by absorbing material (perovskite) and the central (plasmonic) particle (see eqs. (A1,A2)):

$$W^{(a)} = -\oint_{\mathbf{\Sigma}_{OC}} \left\langle \mathbf{S}^{(OC)}(\mathbf{r}) \right\rangle \cdot \widehat{\mathbf{r}}\, da, \tag{A26}$$

where the mean energy flux density $\left\langle \mathbf{S}^{(OC)}(\mathbf{r}) \right\rangle$ trough the surface $\mathbf{\Sigma}_{OC}$ is defined by the EM fields $\mathbf{E}^{out}(\mathbf{r})$, $\mathbf{H}^{out}(\mathbf{r})$ (eq. (A8)) at $r = R_{OC}$:

$$\left\langle \mathbf{S}^{(OC)} \right\rangle = \frac{1}{2}\,\mathrm{Re}([\mathbf{E}^{out} \times \mathbf{H}^{out*}]) \equiv \left\langle \mathbf{S}^{(i)} \right\rangle + \left\langle \mathbf{S}^{(s)} \right\rangle + \langle \mathbf{S}' \rangle\,, \tag{A27}$$

where:

$$\langle \mathbf{S}^{(i)} \rangle \equiv \frac{1}{2}\,\mathrm{Re}\left[\mathbf{E}^{(i)} \times \mathbf{H}^{(i)*}\right] = \widehat{\mathbf{e}}_z I_c \exp\left(-2k_0\,\mathrm{Im}[n] z\right), \tag{A28}$$

$$\langle \mathbf{S}^{(s)} \rangle \equiv \frac{1}{2}\,\mathrm{Re}\left[\mathbf{E}^{(s)} \times \mathbf{H}^{(s)*}\right], \tag{A29}$$

$$\langle \mathbf{S}' \rangle \equiv \frac{1}{2}\left\{\mathrm{Re}(\mathbf{E}^{(i)} \times \mathbf{H}^{(s)*}) + \mathrm{Re}(\mathbf{E}^{(s)} \times \mathbf{H}^{(i)*})\right\}. \tag{A30}$$

Let us note that the $\mathbf{E}^{out} = \mathbf{E}^{i} + \mathbf{E}^{s}$, $\mathbf{H}^{out} = \mathbf{H}^{i} + \mathbf{H}^{s}$ take into account the presence of

the SP, while they fulfil the standard continuity relations at the SP/host interface. The rate of the total energy $W^{(a)}$ absorbed in the volume V_{OC} of the optical cell is:

$$W^{(a)} = -\oint_{\mathbf{\Sigma}_{OC}} \langle S_r^{(i)} \rangle da - \oint_{\mathbf{\Sigma}_{OC}} \langle S_r^{(s)} \rangle da - \oint_{\mathbf{\Sigma}_{OC}} \langle S_r' \rangle da \equiv W^{(i,a)} - W^{(s)} + W', \qquad \text{(A31)}$$

where $W^{(i,a)}$ is the rate of absorption of the incident beam by the absorbing material (perovskite), which fills the whole volume V_{OC} in absence of a scattering particle (see Fig, 3 a)), $W^{(s)}$ is the rate of energy scattered out by the SP and reaching the border of the OC (after propagating in the absorbing medium).

In both cases of absorbing and nonabsorbing host medium, formally the same definitions of the rates of absorbed $W^{(a)}$ and scattered $W^{(s)}$ energies (eq. (A31)) can be used. However, according to our opinion, W' can not be interpreted as the rate of extinction $W^{(ext)}$ in case of absorbing materials hosting the NPs, as accepted in[51,52,59] with the unpleasant (and controversial) consequence that it can be negative (see the inset in Fig. 9 and discussion in Section A4.3). These facts show that the meaning of total extinction rate in case absorbing host requires reconsideration (see Section A4.3).

After calculating the integrals defining $W^{(i,a)}$, $W^{(s)}$, W' (eq. (A31)), it is possible to find the total absorption rate $W^{(a)}$. In spite the task is algebraically rather hard, all the terms $W^{(i,a)}$, $W^{(s)}$ and W' can be calculated strictly.

A4.1 Absorption rate of the incident beam in absence of scattering particle

To find the total energy rate $W^{(a)}$ absorbed in the OC (eq. (A31)), we start with the first contributing term $W^{(i,a)}$, which describes the rate of energy absorbed by the host medium that fills the volume enclosed by $\mathbf{\Sigma}_{OC}$ in case the SP is not present (see Fig. 3 a)). $W^{(i,a)}$ is expressed by the integral of radial component of the Poynting vector $\langle \mathbf{S}^{(i)} \rangle$ (eq. (A28)) over

$\mathbf{\Sigma}_{OC}$:

$$W^{(i,a)} = -\oint_{\mathbf{\Sigma}_{OC}} \langle \mathbf{S}^{(i)}(R_{OC},\theta,\varphi)\rangle \cdot \widehat{\mathbf{r}} R_{OC}^2 \sin\theta d\theta d\phi = \quad \text{(A32)}$$
$$= -I_c R_{OC}^2 \int_0^{2\pi} d\phi \int_0^{\pi} \exp\{-\eta\cos\theta\}\sin\theta\cos\theta d\theta,$$

where the time-averaged Poynting vector $\langle \mathbf{S}^{(i)}\rangle$ is given by eq. (A28) and:

$$\eta \equiv 2k_0 R_{OC}\,\mathrm{Im}[n] = \frac{4\pi R_{OC}\,\mathrm{Im}[n]}{\lambda_0}. \quad \text{(A33)}$$

In[52] the absorption rate $W^{(i,a)}$ of an incident beam given by eq. (A32) is claimed to be overestimated and in calculations, the contribution of energy rate absorbed in the volume V occupied by the central particle was subtracted from $W^{(i,a)}$ (so from the energy budget for OC (eq. (A31)) also). Let us underline that eq. (A1) (or eq. (A26) and the resulting eq. (A31)) are general. By definition, $\mathbf{E}^{(i)}$ and $\mathbf{H}^{(i)}$ in eq. (A28) are solutions of Maxwell equations in a medium without any scatterer present, as explained in[44,60] . Therefore, according to our opinion, the "manual" correction of $W^{(i,a)}$ is not justified.

Using the Integral Calculator[61] tool for calculating the indefinite integral in eq. (A32), we get for $W^{(i,a)}$ (eq. (A32)) the following algebraic expression:

$$W^{(i,a)} = \frac{I_c\lambda_0}{8\pi(\mathrm{Im}[n])^2}\left\{\exp(-\eta)\,(\eta+1) + \exp(\eta)\,(\eta-1)\right\}, \quad \text{(A34)}$$

where I_c accounts for spectral parameters of light illuminating the film (eq. (A11)).

A4.2 Rates of scattered energy at the surface of the optical cell

The rate $W^{(s)}$ of energy scattered by the SP, which reaches the surface $\mathbf{\Sigma}_{OC}$ after attenuation in the host medium, is expressed by the integral of radial component of the Poynting vector

$\langle \mathbf{S}^{(s)} \rangle$ (eq. (A29))) over $\mathbf{\Sigma}_{OC}$ (see the second term in eq. (A31)):

$$W^{(s)} = \int_0^{2\pi}\int_0^{\pi} \langle S_r^{(s)} \rangle R_{OC}^2 \sin\theta d\theta d\phi = \tag{A35}$$
$$= \frac{1}{2} R_{OC}^2 \,\mathrm{Re} \int_0^{2\pi} \left[\int_0^{\pi} \left(E_{s\theta} H_{s\varphi}^* - E_{s\varphi} H_{s\theta}^* \right) \sin\theta d\theta \right] d\phi,$$

where $E_{s\theta}, E_{s\varphi}$ and $H_{s\theta}, H_{s\varphi}$ are the transverse components of the fields $\mathbf{E}^s(\mathbf{r}), \mathbf{H}^s(\mathbf{r})$ at $r = R_{OC}$ which, according to the Lorenz-Mie theory are expressed as appropriate expansions in vector spherical harmonics. The integrals in eq. (A35) can be calculated exactly. Using the results of[52] after correcting the error in sign, we get:

$$W^{(s)} = \frac{2\pi}{|k|^2} I_c \exp\left(-2\,\mathrm{Im}(k)\,(R_{OC} - R)\right) \tag{A36}$$
$$\times \sum_{l=1}^{\infty} (2l+1) \left\{ \left(|a_l|^2 + |b_l|^2 \right) \mathrm{Im}\left(\xi_l(X)\xi_l'^*(X)\right) + \left(|a_l|^2 - |b_l|^2 \right) \frac{\mathrm{Im}(k)}{\mathrm{Re}(k)} \mathrm{Re}\left(\xi_l(X)\xi_l'^*(X)\right) \right\},$$

where $X = kR_{OC}$, I_c (eq. (A11)) accounts for spectral parameters of light illuminating the film.

A4.3 Total rates of energy removed by OC versus "interference" term

The third term W' in eq. (A31), can be calculated as the integral of $\langle S_r' \rangle$ (eq. (A30)) over the surface $\mathbf{\Sigma}_{OC}$:

$$W' = -\int_0^{2\pi}\int_0^{\pi} \langle S'_r \rangle \, R_{OC}^2 \sin\theta d\theta = \tag{A37}$$
$$= -\frac{1}{2} R_{OC}^2 \,\mathrm{Re} \int_0^{2\pi} \left[\int_0^{\pi} \left(E_{i\theta} H^*_{s\varphi} + E_{s\theta} H^*_{i\varphi} - E_{i\varphi} H^*_{s\theta} - E_{s\varphi} H^*_{i\theta} \right) \sin\theta d\theta \right] d\phi.$$

W' can be calculated applying the Lorenz-Mie solutions, and laborious integrations performed in:[52]

$$W' = \frac{2\pi}{|k|^2} I_c \exp\left(-2\,\mathrm{Im}(k)\,(R_{OC} - R)\right) \tag{A38}$$
$$\times \sum_{l=1}^{\infty} (2l+1) \left\{ \mathrm{Re}\,(a_l + b_l)\,\mathrm{Im}\left[F_-(X\right] + \mathrm{Im}\,(a_l + b_l)\,\mathrm{Re}\left[F_-(X)\right] + \right.$$
$$\left. + \mathrm{Re}\,(a_l - b_l)\,\frac{\mathrm{Im}(k)}{\mathrm{Re}(k)}\,\mathrm{Re}\left[F_+(X)\right] - \mathrm{Im}\,(a_l - b_l)\,\frac{\mathrm{Im}(k)}{\mathrm{Re}(k)}\,\mathrm{Im}\left[F_+(X)\right] \right\},$$

where: $F_-(X) \equiv \xi_l(X)\psi_l^{*\prime}(X) - \xi_l'(X)\psi_l^*(X)$ and $F_+(X) \equiv \xi_l(X)\psi_l^{*\prime}(X) + \xi_l'(X)\psi_l^*(X)$, where the argument $X = kR_{OC}$.

W' (eq. (A37)) has no self-reliant physical meaning like in the case of nonabsorbing host medium. For nonabsorbing host, the rate of absorption of the incident beam in absence of the particle $W^{(i,a)} = 0$ (e.g.[39]), and the total scattered energy flux at the surface $\mathbf{\Sigma}_{OC}$ must be the same as those at the surface $\mathbf{\Sigma}$ of the scattering particle: $W^{(a)} + W^{(s)} = w^{(a)} + w^{(s)}$. So, according to the energy budget (eq. (A31)) $W^{(a)} + W^{(s)} = W' = W^{(ext)} = w^{(ext)}$. Let us note however that for the absorbing host medium it is not the case: $W^{(a)} + W^{(s)} = W^{(i,a)} + W'$ (eq. (A31)) with $W^{(i,a)} \neq 0$. Therefore, the rate W' losses the meaning of extinction rate $W^{(ext)}$, which must be the measure of the total energy rate removed from the incident beam by OC:

$$W^{(ext)} \equiv W^{(a)} + W^{(s)} = W^{(i,a)} + W'. \tag{A39}$$

$W^{(ext)}$ defined by eq. (A39) is always positive for all λ_0 and R, in contrary to W' (see the inset in Fig. 10). In the previous papers (e.g.[51–53,59]) W' defined by eq. (A37) was assumed to be the rate of extinction $W^{(ext)}$ in spite that it can be negative.

A5 Illumination of composite film with sunlike light

The results presented in Sections 3 and 4 of the main paper are calculated for flat spectral illumination of the film. Having in mind possible photovoltaic applications of the results of previous sections, we recalculated all the quantities contributing to the net and relative spectral modification of the absorbed energy rates in the perovskite host by of gold and silver SPs (Sections 5 and 6) by replacing the previously assumed flat free-space spectrum of light illuminating the film by sunlight spectrum:[50,57]

$$I_0(\lambda_0) = I_{SUN}(\lambda_0). \tag{A40}$$

with:

$$|E_c(\lambda_0)|^2 = |E_{SUN}(\lambda_0)|^2 \exp\left(-\alpha(\lambda_0)\right) \tag{A41}$$

Solar radiation is represented by harmonic waves with the frequency dependent amplitudes: $|E_{SUN}(\lambda_0)|^2 = I_{SUN}(\lambda_0)/[\frac{k_o \,\mathrm{Re}[n]}{2\omega\mu_0}]$, where $I_{SUN}(\lambda_0)/[\frac{k_o \,\mathrm{Re}[n]}{2\omega\mu_0}]$ is based on the reference base[50] and is illustrated in Fig. 2. The net change $\Delta W^{(a)}_{h,SUN}(\lambda_0)$ in the absorbed energy rate by the host medium, resulting from presence of SP under illumination of the film with sunlight:

$$\Delta W^{(a)}_{h,SUN} = W^{(a)}_{h,SUN} - W^{(i,a)}_{SUN}, \tag{A42}$$

is the analogue of (3) for spectrally flat illumination of the film.

Acknowledgement

The authors would like to thank cordially to Krzysztof A. Kolwas for fruitful discussions and Yevgen Melikhov for reviewing the draft of the manuscript.

References

(1) Foley, J. J.; Ungaro, C.; Sun, K.; Gupta, M. C.; Gray, S. K. Design of emitter structures based on resonant perfect absorption for thermophotovoltaic applications. *Opt. Express* **2015**, *23*, A1373–A1387.

(2) Maier, S. A. *Plasmonics: fundamentals and applications*; Springer Science & Business Media, 2007.

(3) Quinten, M. *Beyond Mie's Theory II–The Generalized Mie Theory*; Wiley Online Library, 2011; pp 317–339.

(4) Wang, Y.; Plummer, E.; Kempa, K. Foundations of plasmonics. *Adv. Phys.* **2011**, *60*, 799–898.

(5) Kolwas, K.; Derkachova, A.; Jakubczyk, D. In *Nanomedicine Tissue Eng. State Art Recent Trends*; Kalarikkal, N., Augustine, R., Oluwafemi, O. S., Joshy, K. S., Sabu, T., Eds.; Apple Acagemic Press, 2016; Chapter 5, pp 141–182.

(6) Kreibig, U.; Vollmer, M. *Optical Properties of Metal Clusters*, springer-v ed.; Springer Series in Materials Science 25; Berlin, Heidelber: Springer, 1995; Vol. 118.

(7) Sönnichsen, C.; Franzl, T.; Wilk, T.; Von Plessen, G.; Feldmann, J. Plasmon resonances in large noble-metal clusters. *New J. Phys.* **2002**, *4*, 93.

(8) Kolwas, K.; Derkachova, A. Damping rates of surface plasmons for particles of size from nano-to micrometers; reduction of the nonradiative decay. *JQSRT* **2013**, *114*, 45–55.

(9) Derkachova, A.; Kolwas, K.; Demchenko, I. Dielectric Function for Gold in Plasmonics Applications: Size Dependence of Plasmon Resonance Frequencies and Damping Rates for Nanospheres. *Plasmonics* **2016**, *11*, 941–951.

(10) Schaadt, D. M.; Feng, B.; Yu, E. T. Enhanced semiconductor optical absorption via surface plasmon excitation in metal nanoparticles. *Appl. Phys. Lett.* **2005**, *86*, 1–3.

(11) Catchpole, K. R.; Polman, A. Plasmonic solar cells. *Opt. Express* **2008**, *16*, 21793–800.

(12) Carretero-Palacios, S.; Calvo, M. E.; Míguez, H. Absorption enhancement in organic–inorganic halide perovskite films with embedded plasmonic gold nanoparticles. *J. Phys. Chem. C* **2015**, *119*, 18635–18640.

(13) Smith, J. G.; Faucheaux, J. A.; Jain, P. K. Plasmon resonances for solar energy harvesting: A mechanistic outlook. *Nano Today* **2015**, *10*, 67–80.

(14) Zhang, W.; Saliba, M.; Stranks, S. D.; Sun, Y.; Shi, X.; Wiesner, U.; Snaith, H. J. Enhancement of perovskite-based solar cells employing core–shell metal nanoparticles. *Nano Lett.* **2013**, *13*, 4505–4510.

(15) Saliba, M.; Zhang, W.; Burlakov, V. M.; Stranks, S. D.; Sun, Y.; Ball, J. M.; Johnston, M. B.; Goriely, A.; Wiesner, U.; Snaith, H. J. Plasmonic-Induced Photon Recycling in Metal Halide Perovskite Solar Cells. *Adv. Funct. Mater.* **2015**, *25*, 5038–5046.

(16) Ross, R. T.; Nozik, A. J. Efficiency of hot-carrier solar energy converters. *J. Appl. Phys.* **1982**, *53*, 3813–3818.

(17) Price, M. B.; Butkus, J.; Jellicoe, T. C.; Sadhanala, A.; Briane, A.; Halpert, J. E.; Broch, K.; Hodgkiss, J. M.; Friend, R. H.; Deschler, F. Hot-carrier cooling and pho-

toinduced refractive index changes in organic-inorganic lead halide perovskites. *Nat. Commun.* **2015**, *6*.

(18) Lin, Q.; Armin, A.; Nagiri, R. C. R.; Burn, P. L.; Meredith, P. Electro-optics of perovskite solar cells. *Nat. Photonics* **2015**, *9*, 106–112.

(19) Zhang, Y.; Yam, C.; Schatz, G. C. Fundamental Limitations to Plasmonic Hot-Carrier Solar Cells. *J. Phys. Chem. Lett.* **2016**, 1852–1858.

(20) Marchuk, K.; Willets, K. A. Localized surface plasmons and hot electrons. *Chem. Phys.* **2014**, *445*, 95–104.

(21) Brongersma, M. L.; Halas, N. J.; Nordlander, P. Plasmon-induced hot carrier science and technology. *Nat. Nanotech.* **2015**, *10*, 25–34.

(22) Wang, S.; Wang, H.; Liu, T.; Huang, Y.; Chen, G.; Wei, H.; Su, X.; Zeng, X.; Xia, Z.; Wen, W. et al. Ascertaining plasmonic hot electrons generation from plasmon decay in hybrid plasmonic modes. *Plasmonics* **2015**, 1–7.

(23) Ng, C.; Cadusch, J. J.; Dligatch, S.; Roberts, A.; Davis, T. J.; Mulvaney, P.; Gómez, D. E. Hot Carrier extraction with plasmonic broadband absorbers. *ACS Nano* **2016**, *10*, 4704–4711.

(24) Cushing, S. K.; Wu, N. Progress and Perspectives of Plasmon-Enhanced Solar Energy Conversion. *J. Phys. Chem. Lett.* **2016**, *7*, 666–675.

(25) Kim, H.-S.; Mora-Sero, I.; Gonzalez-Pedro, V.; Fabregat-Santiago, F.; Juarez-Perez, E. J.; Park, N.-G.; Bisquert, J. Mechanism of carrier accumulation in perovskite thin-absorber solar cells. *Nat. Commun.* **2013**, *4*.

(26) D'Innocenzo, V.; Grancini, G.; Alcocer, M. J.; Kandada, A. R. S.; Stranks, S. D.; Lee, M. M.; Lanzani, G.; Snaith, H. J.; Petrozza, A. Excitons versus free charges in organo-lead tri-halide perovskites. *Nat. Commun.* **2014**, *5*.

(27) Malinkiewicz, O.; Yella, A.; Lee, Y. H.; Espallargas, G. M.; Graetzel, M.; Nazeeruddin, M. K.; Bolink, H. J. Perovskite solar cells employing organic charge-transport layers. *Nat. Photon.* **2014**, *8*, 128–132.

(28) Li, Y.; Meng, L.; Yang, Y. M.; Xu, G.; Hong, Z.; Chen, Q.; You, J.; Li, G.; Yang, Y.; Li, Y. High-efficiency robust perovskite solar cells on ultrathin flexible substrates. *Nat. Commun.* **2016**, *7*.

(29) Marco, N. D.; Zhou, H.; Chen, Q.; Sun, P.; Liu, Z.; Meng, L.; Yao, E.-P.; Liu, Y.; Schiffer, A.; Yang, Y. Guanidinium: a route to enhanced carrier lifetime and open-circuit voltage in hybrid perovskite solar cells. *Nano Lett.* **2016**, *16*, 1009–1016.

(30) Anaya, M.; Lozano, G.; Calvo, M. E.; Zhang, W.; Johnston, M. B.; Snaith, H. J.; Míguez, H. Optical description of mesostructured organic–inorganic halide perovskite solar cells. *J. Phys. Chem. Lett.* **2014**, *6*, 48–53.

(31) Ball, J. M.; Stranks, S. D.; Hörantner, M. T.; Hüttner, S.; Zhang, W.; Crossland, E. J.; Ramirez, I.; Riede, M.; Johnston, M. B.; Friend, R. H. et al. Optical properties and limiting photocurrent of thin-film perovskite solar cells. *Energy Environ. Sci.* **2015**, *8*, 602–609.

(32) Standridge, S. D.; Schatz, G. C.; Hupp, J. T. Distance dependence of plasmon-enhanced photocurrent in dye-sensitized solar cells. *J. Amer. Chem. Soc.* **2009**, *131*, 8407–8409.

(33) Yang, J.; You, J.; Chen, C.-C.; Hsu, W.-C.; Tan, H.-r.; Zhang, X. W.; Hong, Z.; Yang, Y. Plasmonic polymer tandem solar cell. *ACS Nano* **2011**, *5*, 6210–6217.

(34) Brown, M. D.; Suteewong, T.; Kumar, R. S. S.; D'Innocenzo, V.; Petrozza, A.; Lee, M. M.; Wiesner, U.; Snaith, H. J. Plasmonic dye-sensitized solar cells using core-shell metal-insulator nanoparticles. *Nano Lett.* **2011**, *11*, 438–445.

(35) Cole, J. R.; Halas, N. Optimized plasmonic nanoparticle distributions for solar spectrum harvesting. *Appl. Phys. Lett.* **2006**, *89*, 153120.

(36) Derkachova, A.; Kolwas, K. Size dependence of multipolar plasmon resonance frequencies and damping rates in simple metal spherical nanoparticles. *EPJ Spec. Top.* **2007**, *144*, 93–99.

(37) Kolwas, K.; Derkachova, A.; Shopa, M. Size characteristics of surface plasmons and their manifestation in scattering properties of metal particles. *JQSRT* **2009**, *110*, 1490–1501.

(38) Bohren, C. F.; Huffman, D. R. *Absorption and scattering of light by small particles*; Wiley science paperback series; John Wiley & Sons, 1983.

(39) Born, M.; Wolf, E. *Principles of optics: electromagnetic theory of propagation, interference and diffraction of light*; Cambridge University Press, 1999.

(40) Hergert, W.; Wriedt, T. *The Mie Theory: basics and applications*; Springer, 2012; Vol. 169.

(41) Aden, A. L.; Kerker, M. Scattering of Electromagnetic Waves from Two Concentric Spheres. *J. Appl. Phys.* **1951**, *22*, 1242.

(42) Bhandari, R. Scattering coefficients for a multilayered sphere: analytic expressions and algorithms. *Appl. Opt.* **1985**, *24*, 1960–1967.

(43) Sinzig, J.; Quinten, M. Scattering and absorption by spherical multilayer particles. *Appl. Phys. A* **1994**, *58*, 157–162.

(44) Gouesbet, G.; Gréhan, G. *Generalized Lorenz-Mie Theories*; Springer Science & Business Media, 2011.

(45) Phillips, L. J.; Rashed, A. M.; Treharne, R. E.; Kay, J.; Yates, P.; Mitrovic, I. Z.; Weerakkody, A.; Hall, S.; Durose, K. Dispersion relation data for methylammonium

lead triiodide perovskite deposited on a (100) silicon wafer using a two-step vapour-phase reaction process. *Data in Brief* **2015**, *5*, 926–928.

(46) Perovskite refractive index. `http://refractiveindex.info/?shelf=other&book=CH3NH3PbI3&page=Phillips`, (accessed January 11, 2017).

(47) Hulst, H. C.; van de Hulst, H. C. *Light scattering by small particles*; Courier Corporation, 1957.

(48) Reinhard, B. M.; Siu, M.; Agarwal, H.; Alivisatos, A. P.; Liphardt, J. Calibration of dynamic molecular rulers based on plasmon coupling between gold nanoparticles. *Nano Lett.* **2005**, *5*, 2246–2252.

(49) Johnson, P. B.; Christy, R.-W. Optical constants of the noble metals. *Phys. Rev. B* **1972**, *6*, 4370.

(50) Reference Solar Spectral Irradiance: ASTM G-173. `http://rredc.nrel.gov/solar/spectra/am1.5/ASTMG173/ASTMG173.html`, (accessed January 11,2017).

(51) Mundy, W. C.; Roux, J. A.; Smith, A. M. Mie scattering by spheres in an absorbing medium. *JOSA* **1974**, *64*, 1593–1597.

(52) Quinten, M.; Rostalski, J. Lorenz-Mie Theory for Spheres Immersed in an absorbing host medium. *Part. Part. Sys. Char.* **1996**, *13*, 89–96.

(53) Fu, Q.; Sun, W. Mie theory for light scattering by a spherical particle in an absorbing medium. *Appl. Opt.* **2001**, *40*, 1354–1361.

(54) Sudiarta, I. W.; Chylek, P. Mie-scattering formalism for spherical particles embedded in an absorbing medium. *JOSA A* **2001**, *18*, 1275–1278.

(55) Yang, P.; Gao, B.-C.; Wiscombe, W. J.; Mishchenko, M. I.; Platnick, S. E.; Huang, H.-L.; Baum, B. A.; Hu, Y. X.; Winker, D. M.; Tsay, S.-C. Inherent and apparent scattering

properties of coated or uncoated spheres embedded in an absorbing host medium. *Appl. Opt.* **2002**, *41*, 2740–2759.

(56) Videen, G.; Sun, W. Yet another look at light scattering from particles in absorbing media. *Appl. Opt.* **2003**, *42*, 6724–6727.

(57) Solar spectrum calculator. `https://www2.pvlighthouse.com.au/calculators/solarspectrumcalculator/solarspectrumcalculator.aspx`, (accessed January 11, 2017).

(58) Mishchenko, M. I. Electromagnetic scattering by a fixed finite object embedded in an absorbing medium. *Opt. Express* **2007**, *15*, 13188–13202.

(59) Lebedev, A.; Gartz, M.; Kreibig, U.; Stenzel, O. Optical extinction by spherical particles in an absorbing medium: application to composite absorbing films. *EPJ D* **1999**, *6*, 365–373.

(60) Mishchenko, M. I. *Electromagnetic scattering by particles and particle groups: an introduction*; Cambridge University Press, 2014.

(61) Scherfgen, D. Integral Calculator. 2017; `http://www.integral-calculator.com`, (accessed January 11, 2017).

Graphical TOC Entry